What Do You See in Common? Learning Hierarchical Prototypes over Tree-of-Life to Discover Evolutionary Traits

Anonymous Author(s)
Affiliation
Address
email

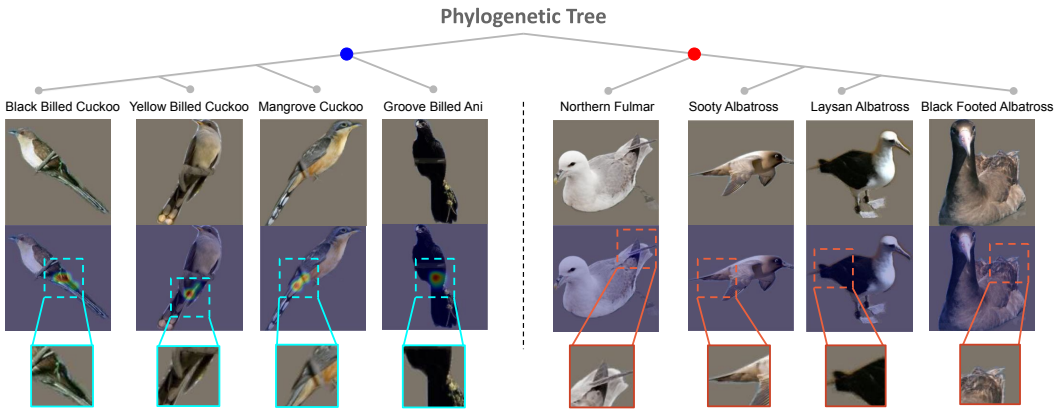

Figure 1: Sample images of bird species with zoomed-in views of learned prototypes along with their associated score maps. We consider the problem of finding evolutionary traits common to a group of species derived from the same ancestor (blue) that are absent in other species from a different ancestor (red). We can infer that descendants of the blue node share a common trait: *long tail*, absent from descendants of the red node.

Abstract

A grand challenge in biology is to discover evolutionary traits—features of organisms common to a group of species with a shared ancestor in the tree of life (also referred to as phylogenetic tree). With the growing availability of image repositories in biology, there is a tremendous opportunity to discover evolutionary traits directly from images in the form of a hierarchy of prototypes. However, current prototype-based methods are mostly designed to operate over a flat structure of classes and face several challenges in discovering hierarchical prototypes, including the issue of learning over-specific features at internal nodes. To overcome these challenges, we introduce the framework of **H**ierarchy aligned **Com**monality through **P**rototypical **Net**works **(HComP-Net)**. We empirically show that HComP-Net learns prototypes that are accurate, semantically consistent, and generalizable to unseen species in comparison to baselines on birds, butterflies, and fishes datasets.

1 Introduction

A central goal in biology is to discover the observable characteristics of organisms, or *traits* (e.g., beak color, stripe pattern, and fin curvature), that help in discriminating between species and understanding

Submitted to 38th Conference on Neural Information Processing Systems (NeurIPS 2024). Do not distribute.

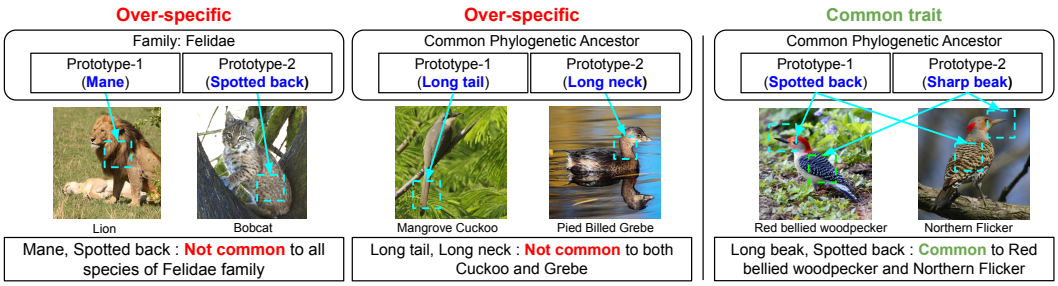

Figure 2: Examples to illustrate the problem of learning "over-specific" prototypes at internal nodes, which only cover one descendant species of the node instead of learning prototypes *common* to all descendants.

how organisms evolve and adapt to their environment [1]. For example, discovering traits inherited by a group of species that share a common ancestor on the tree of life (also referred to as the *phylogenetic tree*, see Figure 1) is of great interest to biologists to understand how organisms diversify and evolve [2]. The measurement of such traits with evolutionary signals, termed *evolutionary traits*, is not straightforward and often relies on subjective and labor-intensive human expertise and definitions [3, 4], hindering rapid scientific advancement [5].

With the growing availability of large-scale image repositories in biology containing millions of images of organisms [6, 7, 8], there is an opportunity for machine learning (ML) methods to discover evolutionary traits automatically from images [5, 9]. This is especially true in light of recent advances in the field of explainable ML, such as the seminal work of ProtoPNet [10] and its variants [11, 12, 13] which find representative patches in training images (termed *prototypes*) capturing discriminatory features for every class. We can thus cast the problem of discovering evolutionary traits into asking the following question: *what image features or prototypes are common across a group of species with a shared ancestor in the tree of life that are absent in species with a different shared ancestor?*

For example, in Figure 1, we can see that the four species of birds on the left descending from the blue node show the common feature of having "long tails," unlike any of the descendant species of the red node. Learning such common features at every internal node as a hierarchy of prototypes can help biologists generate novel hypotheses of species diversification (e.g., the splitting of blue and red nodes) and accumulation of evolutionary trait changes.

Despite the success of ProtoPNet [10] and its variants in learning prototypes over a flat structure of classes, applying them to discover a hierarchy of prototypes is challenging for three main reasons. *First*, existing methods that learn multiple prototypes for every class are prone to learning "over-specific" prototypes at internal nodes of a tree, which cover only one (or a few) of its descendant species. Figure 2 shows a few examples to illustrate the concept of over-specific prototypes. Consider the problem of learning prototypes common to descendant species of the Felidae family: Lion and Bobcat. If we learn one prototype focusing on the feature of the mane (specific only to Lion) and another prototype focusing on the feature of spotted back (specific only to Bobcat), then these two prototypes taken together can classify all images from the Felidae family. However, they do not represent *common* features shared between Lion and Bobcat and hence are not useful for discovering evolutionary traits. Such over-specific prototypes should be instead pushed down to be learned at lower levels of the tree (e.g., the species leaf nodes of Lion and Bobcat).

Second, while existing methods such as ProtoPShare [11], ProtoPool [12], and ProtoTree [13] allow prototypes to be shared across classes for re-usability and sparsity, in the problem of discovering evolutionary traits, we want to learn prototypes at an internal node n that are not just shared across all it descendant species but are also absent in the *contrasting set* of species (i.e., species descending from sibling nodes of n representing alternate paths of diversification). *Third*, at higher levels of the tree, finding features that are common across a large number of diverse species is challenging [14, 15]. In such cases, we should be able to abstain from finding common prototypes without hampering accuracy at the leaf nodes—a feature missing in existing methods.

To address these challenges, we present **H**ierarchy aligned **Com**monality through **P**rototypical **Net**works (**HComP-Net**), a framework to learn hierarchical prototypes over the tree of life for discovering evolutionary traits. Here are the main contributions of our work:

1. HComP-Net learns common traits shared by all descendant species of an internal node and avoids the learning of over-specific prototypes in contrast to baseline methods using a novel *overspecificity loss*.
2. HComP-Net uses a novel *discriminative loss* to ensure that the prototypes learned at an internal node are absent in the contrasting set of species with different ancestry.
3. HComP-Net includes a novel *masking module* to allow for the exclusion of over-specific prototypes at higher levels of the tree without hampering classification performance.
4. We empirically show that HComP-Net learns prototypes that are accurate, semantically consistent, and generalizable to unseen species compared to baselines on data from 190 species of birds (CUB-200-2011 dataset) [8], 38 species of fishes [9], and 30 species of butterflies [16]. We show the ability of HComP-Net to generate novel hypotheses about evolutionary traits at different levels of the phylogenetic tree of organisms.

2 Related Works

One of the seminal lines of work in the field of prototype-based interpretability methods is the framework of ProtoPNet [10] that learns a set of "prototypical patches" from training images of every class to enable case-based reasoning. Following this work, several variants have been developed such as ProtoPShare [11], ProtoPool [12], ProtoTree [13], and HPnet [17] suiting to different interpretability requirements. Among all these approaches, our work is closely related to HPnet [17], the hierarchical extension of ProtoPNet that learns a prototype layer for every parent node in the tree. Despite sharing a similar motivation as our work, HPnet is not designed to avoid the learning of over-specific prototypes or to abstain from learning common prototypes at higher levels of the tree.

Another related line of work is the framework of PIPNet [18], which uses self-supervised learning methods to reduce the "semantic gap" [19, 20] between the latent space of prototypes and the space of images, such that the prototypes in latent space correspond to the same visual concept in the image space. In HComP-Net, we build upon the idea of self-supervised learning introduced in PIPNet to learn semantically consistent hiearchy of prototypes. Our work is also related to ProtoTree [13], which structures the prototypes as nodes in a decision tree to offer more granular interpretability. However, ProtoTree differs from our work in that it learns the tree-based structure of prototypes automatically from data and cannot handle a known hierarchy. Moreover, the prototypes learned in ProtoTree are purely discriminative and allow for negative reasoning, which is not aligned with our objective of finding common traits of descendant species.

Other related works that focus on finding shared features are ProtoPShare [11] and ProtoPool [12]. Both approaches aim to find common features among classes, but their primary goal is to reduce the prototype count by exploiting similarities among classes, leading to a sparser network. This is different from our goal of finding a hiearchy of prototypes to find evolutionary traits common to a group of species (that are absent from other species).

Outside the realm of prototype-based methods, the framework of Phylogeny-guided Neural Networks (PhyloNN) [9] shares a similar motivation as our work to discover evolutionary traits by representing biological images in feature spaces structured by tree-based knowledge (i.e., phylogeny). However, PhyloNN primarily focuses on the tasks of image generation and translation rather than interpretability. Additionally, PhyloNN can only work with discretized trees with fixed number of ancestor levels per leaf node, unlike our work that does not require any discretization of the tree.

3 Proposed Methodology

3.1 HComP-Net Model Architecture

Given a phylogenetic tree with N internal nodes, the goal of HComP-Net is to jointly learn a set of prototype vectors $\mathbf{P_n}$ for every internal node $n \in \{1, \ldots, N\}$. Our architecture as shown in Figure 3 begins with a CNN that acts as a common feature extractor $f(x;\theta)$ for all nodes, where θ represents the learnable parameters of f. f converts an image x into a latent representation $Z \in \mathbb{R}^{H\times W\times C}$, where each "patch" at location (h, w) is, $\mathbf{z}_{\text{h,w}} \in \mathbb{R}^C$. Following the feature extractor, for every node n, we initialize a set of K_n prototype vectors $\mathbf{P_n} = \{\mathbf{p_i}\}_{i=1}^{K_n}$, where $\mathbf{p_i} \in \mathbb{R}^C$. Here, the number of

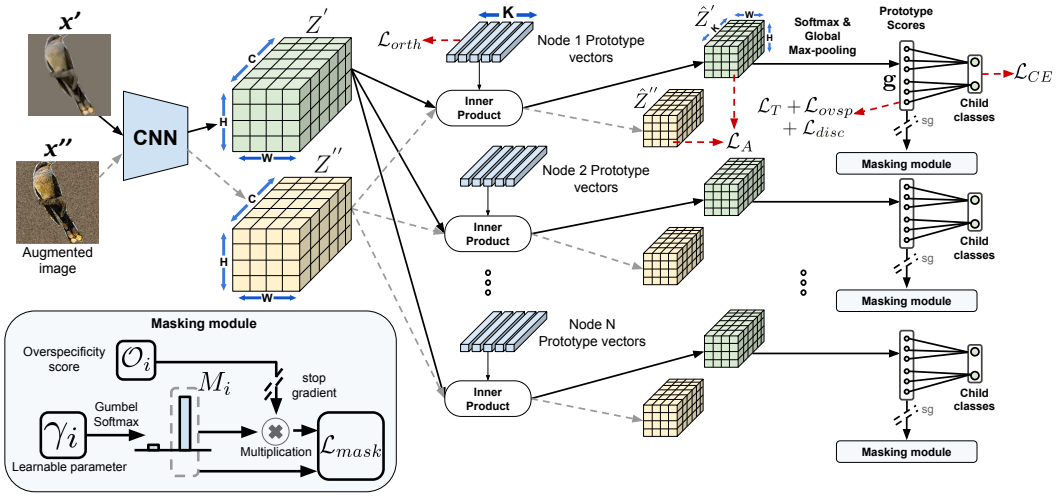

Figure 3: Schematic illustration of HComP-Net model architecture.

prototypes K_n learned at node n varies in proportion to the number of children of node n, with β as the proportionality constant, i.e., at each node n we assign β prototypes for every child node. To simplify notations, we drop the subscript n in $\mathbf{P_n}$ and K_n while discussing the operations occurring in node n.

We consider the following sequence of operations at every node n. We first compute the similarity score between every prototype in $\mathbf{P}$ and every patch in Z. This results in a matrix $\hat{Z} \in \mathbb{R}^{H \times W \times K}$, where every element represents a similarity score between image patches and prototype vectors. We apply a softmax operation across the K channels of $\hat{Z}$ such that the vector $\hat{\mathbf{z}}_{\mathrm{h,w}} \in \mathbb{R}^K$ at spatial location (h, w) in $\hat{Z}$ represents the probability that the corresponding patch $\mathbf{z}_{\mathrm{h,w}}$ is similar to the K prototypes. Furthermore, the i^{th} channel of $\hat{Z}$ serves as a prototype score map for the prototype vector $\mathbf{p_i}$, indicating the presence of $\mathbf{p_i}$ in the image. We perform global max-pooling across the spatial dimensions $H \times W$ of $\hat{Z}$ to obtain a vector $\mathbf{g} \in \mathbb{R}^K$, where the i^{th} element represents the highest similarity score of the prototype vector $\mathbf{p_i}$ across the entire image. $\mathbf{g}$ is then fed to a linear classification layer with weights ϕ to produce the final classification scores for every child node of node n. We restrict the connections in the classification layer so that every child node n_c is connected to a distinct set of β prototypes, to ensure that every prototype uniquely maps to a child node. ϕ is restricted to be non-negative to ensure that the classification is done solely through positive reasoning, similar to the approach used in PIP-Net [18]. We borrow the regularization scheme of PIP-Net to induce sparsity in ϕ by computing the logit of child node n_c as $\log((\mathbf{g}\phi)^2 + 1)$. $\mathbf{g}$ and ϕ here are again unique to each node.

3.2 Loss Functions Used to Train HComP-Net

Contrastive Losses for Learning Hierarchical Prototypes: PIP-Net [18] introduced the idea of using self-supervised contrastive learning to learn semantically meaningful prototypes. We build upon this idea in our work to learn semantically meaningful hierarchical prototypes at every node in the tree as follows. For every input image $\mathbf{x}$, we pass in two augmentations of the image, $\mathbf{x}'$ and $\mathbf{x}''$ to our framework. The prototype score maps for the two augmentations, $\hat{Z}'$ and $\hat{Z}''$, are then considered as positive pairs. Since $\hat{\mathbf{z}}_{\mathrm{h,w}} \in \mathbb{R}^K$ represents the probabilities of patch $\mathbf{z}_{\mathrm{h,w}}$ being similar to the prototypes from $\mathbf{P}$, we align the probabilities from the two augmentations $\hat{\mathbf{z}}'_{\mathrm{h,w}}$ and $\hat{\mathbf{z}}''_{\mathrm{h,w}}$ to be similar using the following alignment loss:

$$\mathcal{L}_A = -\frac{1}{HW} \sum_{(h,w) \in H \times W} \log(\hat{\mathbf{z}}'_{\mathbf{h,w}} \cdot \hat{\mathbf{z}}''_{\mathbf{h,w}}) \tag{1}$$

Since $\sum_{i=1}^{K} \hat{\mathbf{z}}_{\mathbf{h,w,i}} = 1$ due to softmax operation, $\mathcal{L}_A$ is minimum (i.e., $\mathcal{L}_A = 0$) when both $\hat{\mathbf{z}}'_{\mathbf{h,w}}$ and $\hat{\mathbf{z}}''_{\mathbf{h,w}}$ are identical one-hot encoded vectors. A trivial solution that minimizes $\mathcal{L}_A$ is when all

patches across all images are similar to the same prototype. To avoid such representation collapse, we use the following tanh-loss $\mathcal{L}_T$ of PIP-Net [18], which serves the same purpose as uniformity losses in [21] and [22]:

$$\mathcal{L}_T = -\frac{1}{K}\sum_{i=1}^{K}\log(\tanh(\sum_{b=1}^{B}\mathbf{g_{b,i}})), \tag{2}$$

where $\mathbf{g_{b,i}}$ is the prototype score for prototype i with respect to image b of mini-batch. $\mathcal{L}_T$ encourages each prototype $\mathbf{p_i}$ to be activated at least once in a given mini-batch of B images, thereby helping to avoid the possibility of representation collapse. The use of $\tanh$ ensures that only the presence of a prototype is taken into account and not its frequency.

Over-specificity Loss: To achieve the goal of learning prototypes common to all descendant species of an internal node, we introduce a novel loss, termed *over-specificity loss* $\mathcal{L}_{ovsp}$ that avoids learning over-specific prototypes at any node n. $\mathcal{L}_{ovsp}$ is formulated as a modification of the tanh-loss such that prototype $\mathbf{p_i}$ is encouraged to be activated at least once in every one of the descendant species $d \in \{1, \ldots, D_i\}$ of its corresponding child node in the mini-batch of images fed to the model, as follows:

$$\mathcal{L}_{ovsp} = -\frac{1}{K}\sum_{i=1}^{K}\sum_{d=1}^{D_i}\log(\tanh(\sum_{b\in B_d}\mathbf{g_{b,i}})), \tag{3}$$

where B_d is the subset of images in the mini-batch that belong to species d.

Discriminative loss: In order to ensure that a learned prototype for a child node n_c is not activated by any of its *contrasting set* of species (i.e., species that are descendants of child nodes of n other than n_c), we introduce another novel loss function, $\mathcal{L}_{disc}$, defined as follows:

$$\mathcal{L}_{disc} = \frac{1}{K}\sum_{i=1}^{K}\sum_{d\in\widetilde{D_i}}\max_{b\in B_d}(\mathbf{g_{b,i}}), \tag{4}$$

where $\widetilde{D_i}$ is the contrasting set of all descendant species of child nodes of n other than n_c. This is similar to the seperation loss used in other prototype-based methods such as [10], [13], and [23].

Orthogonality loss: We also apply kernel orthogonality as introduced in [24] to the prototype vectors at every node n, so that the learned prototypes are orthogonal and capture diverse features:

$$\mathcal{L}_{orth} = \|\hat{\mathbf{P}}\hat{\mathbf{P}}^\top - I\|_F^2 \tag{5}$$

where $\hat{\mathbf{P}}$ is the matrix of normalized prototype vectors of size $C \times K$, I is an identity matrix, and $\|.\|_F^2$ is the Frobenius norm. Each prototype $\hat{\mathbf{p}}_\mathbf{i}$ in $\hat{\mathbf{P}}$ is normalized as, $\hat{\mathbf{p}}_\mathbf{i} = \frac{\mathbf{p_i}}{\|\mathbf{p_i}\|}$.

Classification loss: Finally, we apply cross entropy loss for classification at each internal node as follows:

$$\mathcal{L}_{CE} = -\sum_{b}^{B} y_b \log(\hat{y}_b) \tag{6}$$

where y is ground truth label and $\hat{y}$ is the prediction at every node of the tree.

3.3 Masking Module to Identify Over-specific Prototypes

We employ an additional masking module at every node n to identify over-specific prototypes without hampering their training. The learned mask for prototype $\mathbf{p_i}$ simply serves as an indicator of whether $\mathbf{p_i}$ is over-specific or not, enabling our approach to abstain from finding common prototypes if there are none, especially at higher levels of the tree. To obtain the mask values, we first calculate the over-specificity score for prototype $\mathbf{p_i}$ as the product of the maximum prototype scores obtained across all images in the mini-batch belonging to every descendant species d as:

$$\mathcal{O}_i = -\prod_{d=1}^{D_i}\max_{(b\in B_d)}(\mathbf{g_{b,i}}) \tag{7}$$

where $\mathbf{g_{b,i}}$ is the prototype score for prototype $\mathbf{p_i}$ with respect to image b of mini-batch and B_d is the subset of images in the mini-batch that belong to descendant species d. Since $\mathbf{g_{b,i}}$ takes a value between 0 to 1 due to the softmax operation, $\mathcal{O}_i$ ranges from -1 to 0, where -1 denotes least

over-specificity and 0 denotes the most over-specificity. The multiplication of the prototype scores ensures that even when the score is less with respect to only one descendant species, the prototype will be assigned a high over-specificity score (close to 0).

As shown in Figure 3, $\mathcal{O}_i$ is then fed into the masking module, which includes a learned mask value M_i for every prototype $\mathbf{p_i}$. We generate M_i from a Gumbel-softmax distribution [25] so that the values are skewed to be very close to either 0 or 1, i.e., $M_i = \text{Gumbel-Softmax}(\gamma_i, \tau)$, where γ_i are the learnable parameters of the distribution and τ is temperature. We then compute the masking loss, $\mathcal{L}_{mask}$, as:

$$\mathcal{L}_{mask} = \sum_{i=1}^{K} (\lambda_{mask} M_i \circ \texttt{stopgrad}(\mathcal{O}_i) + \lambda_{L_1} \|M_i\|_1) \tag{8}$$

where λ_{mask} and λ_{L_1} are trade-off coefficients, $\|.\|_1$ is the L_1 norm added to induce sparsity in the masks, and `stopgrad` represents the stop gradient operation applied over $\mathcal{O}_i$ to ensure that the gradient of $\mathcal{L}_{mask}$ does not flow back to the learning of prototype vectors and impact their training. Note that *the learned masks are not used for pruning the prototypes during training*, they are only used during inference to determine which of the learned prototypes are over-specific and likely to not represent evolutionary traits. Therefore, even if all the prototypes are identified as over-specific by the masking module at an internal node, it will not affect the classification performance at that node.

3.4 Training HComP-Net

We first pre-train the prototypes at every internal node in a self-supervised learning manner using alignment and tanh-losses as $\mathcal{L}_{SS} = \lambda_A \mathcal{L}_A + \lambda_T \mathcal{L}_T$. We then fine-tune the model using the following combined loss: $(\lambda_{CE}\mathcal{L}_{CE} + \mathcal{L}_{SS} + \lambda_{ovsp}\mathcal{L}_{ovsp} + \lambda_{disc}\mathcal{L}_{disc} + \lambda_{orth}\mathcal{L}_{orth} + \mathcal{L}_{mask})$, where λ's are trade-off parameters. Note that the loss is applied over every node in the tree. We show an ablation of key loss terms in our framework in Table 6 in the Supplementary Section.

4 Experimental Setup

Dataset: In our experiments, we primarily focus on the 190 species of birds (**Bird**) from the CUB-200-2011 [8] dataset for which the phylogenetic relationship [26] is known. The tree is quite large with a total of 184 internal nodes. We removed the background from the images to avoid the possibility of learning prototypes corresponding to background information such as the bird's habitat as we are only interested in the traits corresponding to the body of the organism. We also apply our method on a fish dataset with 38 species (**Fish**) [9] along with its associated phylogeny [9] and 30 subspecies of Heliconius butterflies (**Butterfly**) from the Jiggins Heliconius Collection dataset [16] collected from various sources [1] along with its phylogeny [52, 53]. The qualitative results of Butterfly and Fish datasets are provided in the supplementary materials. The complete details of hyper-parameter settings and training strategy are also provided in the Supplementary Section E.

Baselines: We compare HComP-Net to ResNet-50 [54], INTR (Interpretable Transformer) [55] and HPnet [17]. For HPnet, we used the same hyperparameter settings and training strategy as used by ProtoPNet for CUB-200-2011 dataset. For a fair comparison, we also set the number of prototypes for each child in HPnet to be equal to 10 similar to our implementation. We follow the same training strategy as provided by ProtoPNet for CUB-200-2011 dataset.

5 Results

5.1 Fine-grained Accuracy

Similar to HPnet [17], we calculate the fine-grained accuracy for each leaf node by calculating the path probability over every image. During inference, the final probability for leaf class Y given an image X is calculated as, $P(Y|X) = P(Y^{(1)}, Y^{(2)}, ..., Y^{(L)}|X) = \prod_{l=1}^{L} P(Y^{(l)}|X)$, where $P(Y^{(l)}|X)$ is the probability of assigning image X to a node at level l, and L is the depth of the leaf node. Every image is assigned to the leaf class with maximum path probability, which is used to compute the fine-grained accuracy. The comparison of the fine-grained accuracy calculated for

[1] Sources: [27, 28, 29, 30, 31, 32, 33, 34, 35, 36, 37, 38, 39, 40, 41, 42, 43, 44, 45, 46, 47, 48, 49, 50, 51]

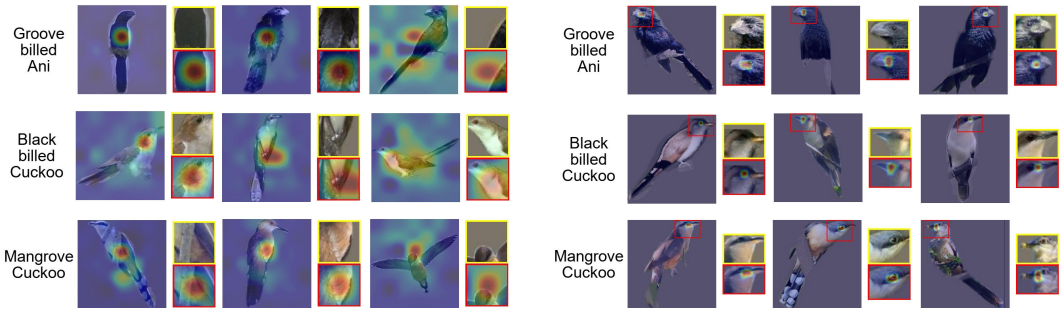

(a) HPnet (b) HComP-Net

Figure 4: Comparing the part consistency of HPnet and HComP-Net for their prototype learned at an internal node in the bird dataset that corresponds to 3 descendant species (names shown on the rows). For every species, we are visualizing the top-3 images with highest prototype score for both HPnet and HComP-Net, shown as the four columns with zoomed in views of their discovered prototypes. We can see that *HPnet highlights varying parts of the bird* across the 3 species and across multiple images of the same species, making it difficult to associate a consistent semantic meaning to its learned prototype. In contrast, *HComP-Net consistently highlights the head region* of the bird across all four species and their images.

HComP-Net and the baselines are given in Table 1. We can see that HComP-Net performs better than the other interpretable methods, such as INTR and HPNet, and is also able to nearly match the performance of non-interpretable models, such as ResNet-50, even outperforming it for the Fish and Butterfly dataset. This shows the ability of our proposed framework to achieve competitive classification accuracy along with serving the goal of discovering evolutionary traits.

Table 1: % Accuracy

Model	Hierarchy	Bird	Butterfly	Fish
ResNet-50	No	**74.18**	95.76	86.63
INTR		69.22	95.53	86.73
HPnet	Yes	36.18	94.69	77.51
HComP-Net		70.01	**97.35**	**90.80**

Table 2: % Accuracy (on unseen species)

Species Name	HComP-Net	HPnet
Fish Crow	53.33	10.55
Rock Wren	53.33	10.22
Indigo Bunting	96.67	49.2
Bohemian Waxwing	70.00	44.9

5.2 Generalizing to Unseen Species in the Phylogeny

We analyze the performance of HComP-Net in generalizing to unseen species that the model hasn't seen during training. The biological motivation for this experiment is to evaluate if HComP-Net can situate newly discovered species at its appropriate position in the phylogeny by identifying its common ancestors shared with the known species. An added advantage of our work is that along with identifying the ancestor of an unseen species, we can also identify the common traits shared by the novel species with known species in the phylogeny. Since unseen species cannot be classified to the finest levels (i.e., up to the leaf node corresponding to the unseen species), we analyze the ability of HComP-Net to classify unseen species accurately up to one level above the leaf level in the hierarchy. With this consideration, the final probability of an unseen species for a given image is calculated as, $P(Y|X_{unseen}) = P(Y^{(1)}, Y^{(2)}, ..., Y^{(L-1)}|X) = \prod_{l=1}^{L-1} P(Y^{(l)}|X)$. Note that we leave out the class probability at the L^{th} level, since we do not take into account the class probability of the leaf level. We leave four species from the Bird training set and calculate their accuracy during inference in Table 2. We can see that HComP-Net is able to generalize better than HPnet for all four species.

5.3 Analyzing the Semantic Quality of Prototypes

Following the method introduced in PIPNet [18], we assess the semantic quality of our learned prototypes by evaluating their part purity. A prototype with high part purity (close to 1) is one that consistently highlights the same image region in the score maps (corresponding to consistent local features such as the eye or wing of a bird) across images belonging to the same class. The part

purity is calculated using the part locations of 15 parts that are provided in the CUB dataset. For each prototype, we take the top-10 images from each leaf descendant. We consider the 32×32 image patch that is centered around the max activation location of the prototype from the top-10 images. With these top-10 image patches, we calculate for each part how frequently the part is present inside the image patch. For example, a part that is found inside the image patch 8 out of 10 times is given a score of 0.8. In PIP-Net, the highest value among the values calculated for each part is given as the part purity of the prototype. In our approach, since we are dealing with a hierarchy and taking the top-10 from each leaf descendant, a particular part, let's say the eye, might have a score of 0.5 for one leaf descendant and 0.7 for a different leaf descendant. Since we want the prototype to represent the same part for all the leaf descendants, we take the lowest score (the weakest link) among all the leaf descendants as the score of the part. By following this method, for a given prototype we can arrive at a value for each part and finally take the maximum among the values as the purity of the prototype. We take the mean of the part purity across all the prototypes and report the results in Table 3 for different ablations of HComP-Net and also HPnet, which is the only baseline method that can learn hierarchical prototypes.

Table 3: Part purity of prototypes on **Bird** dataset.

Model	$\mathcal{L}_{ovsp}$	Masking	Part purity	% masked
HPnet	-	-	0.14 ± 0.09	-
HComP-Net	-	-	0.68 ± 0.22	-
HComP-Net	-	✓	0.75 ± 0.17	21.42%
HComP-Net	✓	-	0.72 ± 0.19	-
HComP-Net	✓	✓	$\mathbf{0.77 \pm 0.16}$	16.53%

We can see that HComP-Net, even without the use of over-specificity loss performs much better than HPnet due to the contrastive learning approach we have adopted from PIPNet [18]. The addition of over-specificity loss improves the part purity because over-specific prototypes tend to have poor part purity for some of the leaf descendants which will affect their overall part purity score. Further, for both ablations with and without over-specificity loss, we apply the masking module and remove masked (over-specific) prototypes during the calculation of part purity. We see that the part purity goes higher by applying the masking module, demonstrating its effectiveness in identifying over-specific prototypes. We further compute the purity of masked-out prototypes and notice that the masked-out prototypes have drastically lower part purity (0.29 ± 0.17) compared to non-masked prototypes (0.77 ± 0.16). An alternative approach to learning the masking module is to identify over-specific prototypes using a fixed global threshold over $\mathcal{O}_i$. We show in Table 9 of Supplementary Section F, that given the right choice of such a threshold, we can identify over-specific prototypes. However, selecting the ideal threshold can be non-trivial. On the other hand, our masking module learns the appropriate threshold dynamically as part of the training process.

Figure 4 visualizes the part consistency of prototypes discovered by HComP-Net in comparison to HPnet for the bird dataset. We can see that HComP-Net is finding a consistent region in the image (corresponding to the head region) across all three descendant species and all images of a species, in contrast to HPnet. Futhermore, thanks to the alignment loss, every patch $\hat{\mathbf{z}}_{\text{h,w}}$ is encoded as nearly a one-hot encoding with respect to the K prototypes which causes the prototype score maps to be highly localized. The concise and focused nature of the prototype score maps makes the interpretation much more effective compared to baselines.

5.4 Analyzing Evolutionary Traits Discovered by HComP-Net

We now qualitatively analyze some of the hypothesized evolutionary traits discovered in the hierarchy of prototypes learned by HComP-Net. Figure 5 shows the hierarchy of prototypes discovered over a small subtree of the phylogeny from Bird (four species) and Fish (three species) dataset. In the visualization of bird prototypes, we can see that the two Pelican species share a consistent region in the learned Prototype labeled 2, which corresponds to the head region of the birds. We can hypothesize this prototype to be capturing the white colored crown common to the two species. On the other hand, Prototype 1 finds the shared trait of similar beak morphology (e.g., sharpness of beaks) across the two Cormorant species. We can see that HComP-Net avoids the learning of over-specific prototypes at internal nodes, which are pushed down to individual leaf nodes, as shown in visualizations of Prototype 3, 4, 5, and 6. Similarly, in the visualization of the fish prototypes, we can see that Prototype 1 is highlighting a specific fin (dorsal fin) of the *Carassius auratus* and *Notropis hudsonius* species, possibly representing their pigmentation and structure, which is noticeably different compared to the contrasting species of *Alosa chrysochloris*. Note that while HComP-Net identifies the common

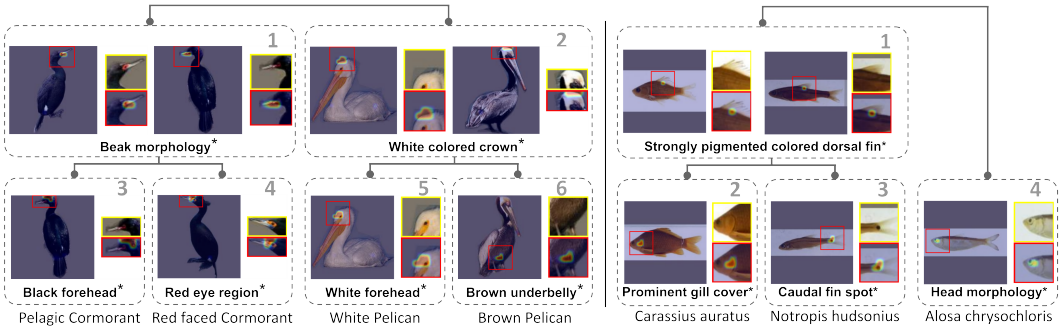

Figure 5: Visualizing the hierarchy of prototypes discovered by HComP-Net for birds and fishes. *Note that the textual descriptions of the hypothesized traits shown for every prototype are based on human interpretation.

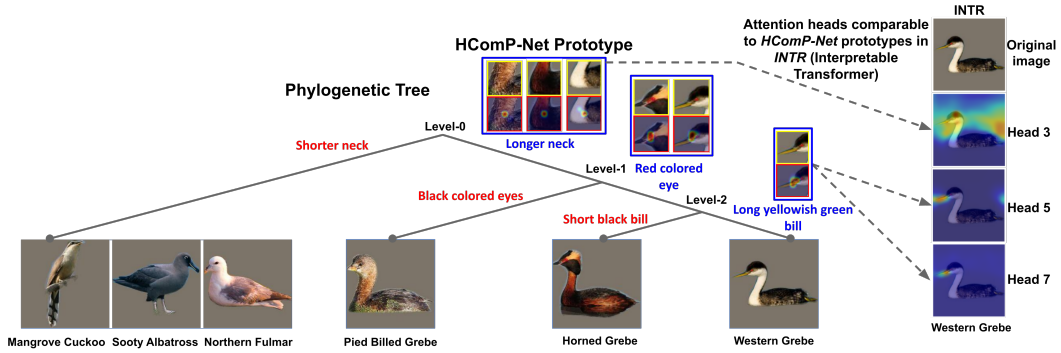

Figure 6: We trace the prototypes learned for Western Grebe at three different levels in the phylogenetic tree (corresponding to different periods of time in evolution). Text in blue is the interpretation of common traits of descendants found by HComP-Net at every ancestor node of Western Grebe.

regions corresponding to each prototype (shown as heatmaps), the textual descriptions of the traits provided in Figure 5 are based on human interpretation.

Figure 6 shows another visualization of the sequence of prototypes learned by HComP-Net for the Western Grebe species at different levels of the phylogeny. We can see that at level 0, we are capturing features closer to the neck region, indicating the likely difference between the length of necks between Grebe species and other species (Cuckoo, Albatross, and Fulmar) that diversify at an earlier time in the process of evolution. At level 1, the prototype is focusing on the eye region, potentially indicating to difference in the color of red and black patterns around the eyes. At level 2, we are differentiating Western Grebe from Horned Grebe based on the feature of bills. We also validate our prototypes by comparing them with the multi-head cross-attention maps learned by INTR [55]. We can see that some of the prototypes discovered by HComP-Net can be mapped to equivalent attention heads of INTR. However, while INTR is designed to produce a flat structure of attention maps, we are able to place these maps on the tree of life. This shows the power of HComP-Net in generating novel hypotheses about how trait changes may have evolved and accumulated across different branches of the phylogeny. Additional visualizations of discovered evolutionary traits for butterfly species and fish species are provided in the supplementary section in Figures 7 to 16.

6 Conclusion

We introduce a novel approach for learning hierarchy-aligned prototypes while avoiding the learning of over-specific features at internal nodes of the phylogenetic tree, enabling the discovery of novel evolutionary traits. Our empirical analysis on birds, fishes, and butterflies, demonstrates the efficacy of HComP-Net over baseline methods. Furthermore, HComP-Net demonstrates a unique ability to generate novel hypotheses about evolutionary traits, showcasing its potential in advancing our understanding of evolution. We discuss the limitations of our work in Supplementary Section I. While we focus on the biological problem of discovering evolutionary traits, our work can be applied in general to domains involving a hierarchy of classes, which can be explored in future research.

References

[1] David Houle and Daniela M Rossoni. Complexity, evolvability, and the process of adaptation. *Annual Review of Ecology, Evolution, and Systematics*, 53, 2022.

[2] Maureen A O'Leary and Seth Kaufman. Morphobank: phylophenomics in the "cloud". *Cladistics*, 27(5):529–537, 2011.

[3] Tiago R Simões, Michael W Caldwell, Alessandro Palci, and Randall L Nydam. Giant taxon-character matrices: quality of character constructions remains critical regardless of size. *Cladistics*, 33(2):198–219, 2017.

[4] Paul C Sereno. Logical basis for morphological characters in phylogenetics. *Cladistics*, 23(6):565–587, 2007.

[5] Moritz D Lürig, Seth Donoughe, Erik I Svensson, Arthur Porto, and Masahito Tsuboi. Computer vision, machine learning, and the promise of phenomics in ecology and evolutionary biology. *Frontiers in Ecology and Evolution*, 9:642774, 2021.

[6] Grant Van Horn, Oisin Mac Aodha, Yang Song, Yin Cui, Chen Sun, Alex Shepard, Hartwig Adam, Pietro Perona, and Serge Belongie. The inaturalist species classification and detection dataset. In *Proceedings of the IEEE conference on computer vision and pattern recognition*, pages 8769–8778, 2018.

[7] Randal A Singer, Kevin J Love, and Lawrence M Page. A survey of digitized data from us fish collections in the idigbio data aggregator. *PloS one*, 13(12):e0207636, 2018.

[8] Catherine Wah, Steve Branson, Peter Welinder, Pietro Perona, and Serge Belongie. The caltech-ucsd birds-200-2011 dataset. 2011.

[9] Mohannad Elhamod, Mridul Khurana, Harish Babu Manogaran, Josef C Uyeda, Meghan A Balk, Wasila Dahdul, Yasin Bakis, Henry L Bart Jr, Paula M Mabee, Hilmar Lapp, et al. Discovering novel biological traits from images using phylogeny-guided neural networks. In *Proceedings of the 29th ACM SIGKDD Conference on Knowledge Discovery and Data Mining*, pages 3966–3978, 2023.

[10] Chaofan Chen, Oscar Li, Daniel Tao, Alina Barnett, Cynthia Rudin, and Jonathan K Su. This looks like that: deep learning for interpretable image recognition. *Advances in neural information processing systems*, 32, 2019.

[11] Dawid Rymarczyk, Łukasz Struski, Jacek Tabor, and Bartosz Zieliński. Protopshare: Prototypical parts sharing for similarity discovery in interpretable image classification. In *Proceedings of the 27th ACM SIGKDD Conference on Knowledge Discovery & Data Mining*, pages 1420–1430, 2021.

[12] Dawid Rymarczyk, Łukasz Struski, Michał Górszczak, Koryna Lewandowska, Jacek Tabor, and Bartosz Zieliński. Interpretable image classification with differentiable prototypes assignment. In *European Conference on Computer Vision*, pages 351–368. Springer, 2022.

[13] Meike Nauta, Ron Van Bree, and Christin Seifert. Neural prototype trees for interpretable fine-grained image recognition. In *Proceedings of the IEEE/CVF Conference on Computer Vision and Pattern Recognition*, pages 14933–14943, 2021.

[14] Luke J Harmon, Jonathan B Losos, T Jonathan Davies, Rosemary G Gillespie, John L Gittleman, W Bryan Jennings, Kenneth H Kozak, Mark A McPeek, Franck Moreno-Roark, Thomas J Near, et al. Early bursts of body size and shape evolution are rare in comparative data. *Evolution*, 64(8):2385–2396, 2010.

[15] Matthew W Pennell, Richard G FitzJohn, William K Cornwell, and Luke J Harmon. Model adequacy and the macroevolution of angiosperm functional traits. *The American Naturalist*, 186(2):E33–E50, 2015.

[16] Christopher Lawrence and Elizabeth G. Campolongo. Heliconius collection (cambridge butterfly), 2024.

[17] Peter Hase, Chaofan Chen, Oscar Li, and Cynthia Rudin. Interpretable image recognition with hierarchical prototypes. In *Proceedings of the AAAI Conference on Human Computation and Crowdsourcing*, volume 7, pages 32–40, 2019.

[18] Meike Nauta, Jörg Schlötterer, Maurice van Keulen, and Christin Seifert. Pip-net: Patch-based intuitive prototypes for interpretable image classification. In *Proceedings of the IEEE/CVF Conference on Computer Vision and Pattern Recognition*, pages 2744–2753, 2023.

[19] Adrian Hoffmann, Claudio Fanconi, Rahul Rade, and Jonas Kohler. This looks like that... does it? shortcomings of latent space prototype interpretability in deep networks. *arXiv preprint arXiv:2105.02968*, 2021.

[20] Sunnie SY Kim, Nicole Meister, Vikram V Ramaswamy, Ruth Fong, and Olga Russakovsky. Hive: Evaluating the human interpretability of visual explanations. In *European Conference on Computer Vision*, pages 280–298. Springer, 2022.

[21] Tongzhou Wang and Phillip Isola. Understanding contrastive representation learning through alignment and uniformity on the hypersphere. In *International Conference on Machine Learning*, pages 9929–9939. PMLR, 2020.

[22] Thalles Silva and Adín Ramírez Rivera. Representation learning via consistent assignment of views to clusters. In *Proceedings of the 37th ACM/SIGAPP Symposium on Applied Computing*, pages 987–994, 2022.

[23] Jiaqi Wang, Huafeng Liu, Xinyue Wang, and Liping Jing. Interpretable image recognition by constructing transparent embedding space. In *Proceedings of the IEEE/CVF International Conference on Computer Vision*, pages 895–904, 2021.

[24] Jiayun Wang, Yubei Chen, Rudrasis Chakraborty, and Stella X Yu. Orthogonal convolutional neural networks. In *Proceedings of the IEEE/CVF conference on computer vision and pattern recognition*, pages 11505–11515, 2020.

[25] Eric Jang, Shixiang Gu, and Ben Poole. Categorical reparameterization with gumbel-softmax. *arXiv preprint arXiv:1611.01144*, 2016.

[26] W. Jetz, G. H. Thomas, J. B. Joy, K. Hartmann, and A. O. Mooers. The global diversity of birds in space and time. *Nature*, 491:444–448, 2012.

[27] Gabriela Montejo-Kovacevich, Eva van der Heijden, Nicola Nadeau, and Chris Jiggins. Cambridge butterfly wing collection batch 10, November 2020.

[28] Patricio A. Salazar, Nicola Nadeau, Gabriela Montejo-Kovacevich, and Chris Jiggins. Sheffield butterfly wing collection - Patricio Salazar, Nicola Nadeau, Ikiam broods batch 1 and 2, November 2020.

[29] Gabriela Montejo-Kovacevich, Chris Jiggins, and Ian Warren. Cambridge butterfly wing collection batch 2, May 2019.

[30] Chris Jiggins, Gabriela Montejo-Kovacevich, Ian Warren, and Eva Wiltshire. Cambridge butterfly wing collection batch 3, May 2019.

[31] Gabriela Montejo-Kovacevich, Chris Jiggins, and Ian Warren. Cambridge butterfly wing collection batch 4, May 2019.

[32] Gabriela Montejo-Kovacevich, Chris Jiggins, Ian Warren, and Eva Wiltshire. Cambridge butterfly wing collection batch 5, May 2019.

[33] Ian Warren and Chris Jiggins. Miscellaneous Heliconius wing photographs (2001-2019) Part 1, February 2019.

[34] Ian Warren and Chris Jiggins. Miscellaneous Heliconius wing photographs (2001-2019) Part 3, February 2019.

[35] Gabriela Montejo-Kovacevich, Chris Jiggins, Ian Warren, and Eva Wiltshire. Cambridge butterfly wing collection batch 6, May 2019.

[36] Chris Jiggins and Ian Warren. Cambridge butterfly wing collection - Chris Jiggins 2001/2 broods batch 1, January 2019.

[37] Chris Jiggins and Ian Warren. Cambridge butterfly wing collection - Chris Jiggins 2001/2 broods batch 2, January 2019.

[38] Joana I. Meier, Patricio Salazar, Gabriela Montejo-Kovacevich, Ian Warren, and Chris Jggins. Cambridge butterfly wing collection - Patricio Salazar PhD wild specimens batch 3, October 2020.

[39] Gabriela Montejo-Kovacevich, Chris Jiggins, and Ian Warren. Cambridge butterfly wing collection batch 1- version 2, May 2019.

[40] Gabriela Montejo-Kovacevich, Chris Jiggins, Ian Warren, Camilo Salazar, Marianne Elias, Imogen Gavins, Eva Wiltshire, Stephen Montgomery, and Owen McMillan. Cambridge and collaborators butterfly wing collection batch 10, May 2019.

[41] Patricio Salazar, Gabriela Montejo-Kovacevich, Ian Warren, and Chris Jiggins. Cambridge butterfly wing collection - Patricio Salazar PhD wild and bred specimens batch 1, December 2018.

[42] Gabriela Montejo-Kovacevich, Chris Jiggins, Ian Warren, and Eva Wiltshire. Cambridge butterfly wing collection batch 7, May 2019.

[43] Patricio Salazar, Gabriela Montejo-Kovacevich, Ian Warren, and Chris Jiggins. Cambridge butterfly wing collection - Patricio Salazar PhD wild and bred specimens batch 2, January 2019.

[44] Erika Pinheiro de Castro, Christopher Jiggins, Karina Lucas da Silva-Brand0̆0e3o, Andre Victor Lucci Freitas, Marcio Zikan Cardoso, Eva Van Der Heijden, Joana Meier, and Ian Warren. Brazilian Butterflies Collected December 2020 to January 2021, February 2022.

[45] Gabriela Montejo-Kovacevich, Chris Jiggins, Ian Warren, and Eva Wiltshire. Cambridge butterfly wing collection batch 8, May 2019.

[46] Gabriela Montejo-Kovacevich, Chris Jiggins, Ian Warren, Eva Wiltshire, and Imogen Gavins. Cambridge butterfly wing collection batch 9, May 2019.

[47] Gabriela Montejo-Kovacevich, Eva van der Heijden, and Chris Jiggins. Cambridge butterfly collection - GMK Broods Ikiam 2018, November 2020.

[48] Gabriela Montejo-Kovacevich, Quentin Paynter, and Amin Ghane. Heliconius erato cyrbia, Cook Islands (New Zealand) 2016, 2019, 2021, September 2021.

[49] Ian Warren and Chris Jiggins. Miscellaneous Heliconius wing photographs (2001-2019) Part 2, February 2019.

[50] Camilo Salazar, Gabriela Montejo-Kovacevich, Chris Jiggins, Ian Warren, and Imogen Gavins. Camilo Salazar and Cambridge butterfly wing collection batch 1, May 2019.

[51] Anniina Mattila, Chris Jiggins, and Ian Warren. University of Helsinki butterfly collection - Anniina Mattila bred specimens, February 2019.

[52] OpenTreeOfLife, Benjamin Redelings, Luna Luisa Sanchez Reyes, Karen A. Cranston, Jim Allman, Mark T. Holder, and Emily Jane McTavish. Open tree of life synthetic tree, 2019.

[53] Francois Michonneau, Joseph W. Brown, and David J. Winter. rotl: an r package to interact with the open tree of life data. *Methods in Ecology and Evolution*, 7(12):1476–1481, 2016.

[54] Kaiming He, Xiangyu Zhang, Shaoqing Ren, and Jian Sun. Deep residual learning for image recognition. In *Proceedings of the IEEE conference on computer vision and pattern recognition*, pages 770–778, 2016.

[55] Dipanjyoti Paul, Arpita Chowdhury, Xinqi Xiong, Feng-Ju Chang, David Carlyn, Samuel Stevens, Kaiya Provost, Anuj Karpatne, Bryan Carstens, Daniel Rubenstein, et al. A simple interpretable transformer for fine-grained image classification and analysis. *arXiv preprint arXiv:2311.04157*, 2023.

[56] Abien Fred Agarap. Deep learning using rectified linear units (relu). *arXiv preprint arXiv:1803.08375*, 2018.

[57] Samuel G Müller and Frank Hutter. Trivialaugment: Tuning-free yet state-of-the-art data augmentation. In *Proceedings of the IEEE/CVF international conference on computer vision*, pages 774–782, 2021.

[58] R. Farrell. Cub-200-2011 segmentations (1.0) [data set], 2024.

NeurIPS Paper Checklist

1. **Claims**

   Question: Do the main claims made in the abstract and introduction accurately reflect the paper's contributions and scope?

   Answer: [Yes]

   Justification: We claim that HComP-Net can generate novel hypotheses for potential evolutionary traits (shared traits among species due to common ancestry in the phylogeny) from image by learning prototypes at each internal node in the phylogenetic tree. We show through various visualizations of the prototypes in Figures 5, 6, and 7 to 16, that the learned prototypes at the internal nodes can identify possible evolutionary traits from images. We also evaluate the improved interpretability of our approach quantitatively in Table 3 by computing part purity metric on Bird dataset.

   Guidelines:

   - The answer NA means that the abstract and introduction do not include the claims made in the paper.
   - The abstract and/or introduction should clearly state the claims made, including the contributions made in the paper and important assumptions and limitations. A No or NA answer to this question will not be perceived well by the reviewers.
   - The claims made should match theoretical and experimental results, and reflect how much the results can be expected to generalize to other settings.
   - It is fine to include aspirational goals as motivation as long as it is clear that these goals are not attained by the paper.

2. **Limitations**

   Question: Does the paper discuss the limitations of the work performed by the authors?

   Answer: [Yes]

   Justification: We discuss the limitations of our work in Supplementary Section I.

   Guidelines:

   - The answer NA means that the paper has no limitation while the answer No means that the paper has limitations, but those are not discussed in the paper.
   - The authors are encouraged to create a separate "Limitations" section in their paper.
   - The paper should point out any strong assumptions and how robust the results are to violations of these assumptions (e.g., independence assumptions, noiseless settings, model well-specification, asymptotic approximations only holding locally). The authors should reflect on how these assumptions might be violated in practice and what the implications would be.
   - The authors should reflect on the scope of the claims made, e.g., if the approach was only tested on a few datasets or with a few runs. In general, empirical results often depend on implicit assumptions, which should be articulated.
   - The authors should reflect on the factors that influence the performance of the approach. For example, a facial recognition algorithm may perform poorly when image resolution is low or images are taken in low lighting. Or a speech-to-text system might not be used reliably to provide closed captions for online lectures because it fails to handle technical jargon.
   - The authors should discuss the computational efficiency of the proposed algorithms and how they scale with dataset size.
   - If applicable, the authors should discuss possible limitations of their approach to address problems of privacy and fairness.
   - While the authors might fear that complete honesty about limitations might be used by reviewers as grounds for rejection, a worse outcome might be that reviewers discover limitations that aren't acknowledged in the paper. The authors should use their best judgment and recognize that individual actions in favor of transparency play an important role in developing norms that preserve the integrity of the community. Reviewers will be specifically instructed to not penalize honesty concerning limitations.

3. **Theory Assumptions and Proofs**

   Question: For each theoretical result, does the paper provide the full set of assumptions and a complete (and correct) proof?

   Answer: [NA]

   Justification: The assumptions made in our work do not require explicit theoretical proofs. Instead, for the key loss terms that we introduce in this work, we provide ablation results in Supplementary Table 6 to show empirically the importance of each component.

   Guidelines:

   - The answer NA means that the paper does not include theoretical results.
   - All the theorems, formulas, and proofs in the paper should be numbered and cross-referenced.
   - All assumptions should be clearly stated or referenced in the statement of any theorems.
   - The proofs can either appear in the main paper or the supplemental material, but if they appear in the supplemental material, the authors are encouraged to provide a short proof sketch to provide intuition.
   - Inversely, any informal proof provided in the core of the paper should be complemented by formal proofs provided in appendix or supplemental material.
   - Theorems and Lemmas that the proof relies upon should be properly referenced.

4. **Experimental Result Reproducibility**

   Question: Does the paper fully disclose all the information needed to reproduce the main experimental results of the paper to the extent that it affects the main claims and/or conclusions of the paper (regardless of whether the code and data are provided or not)?

   Answer: [Yes]

   Justification: We provide details of hyperparameters in Supplementary Section E. Furthermore, we also provide the full code, data, and necessary data preprocessing pipelines to reproduce all the experiments.

   Guidelines:

   - The answer NA means that the paper does not include experiments.
   - If the paper includes experiments, a No answer to this question will not be perceived well by the reviewers: Making the paper reproducible is important, regardless of whether the code and data are provided or not.
   - If the contribution is a dataset and/or model, the authors should describe the steps taken to make their results reproducible or verifiable.
   - Depending on the contribution, reproducibility can be accomplished in various ways. For example, if the contribution is a novel architecture, describing the architecture fully might suffice, or if the contribution is a specific model and empirical evaluation, it may be necessary to either make it possible for others to replicate the model with the same dataset, or provide access to the model. In general. releasing code and data is often one good way to accomplish this, but reproducibility can also be provided via detailed instructions for how to replicate the results, access to a hosted model (e.g., in the case of a large language model), releasing of a model checkpoint, or other means that are appropriate to the research performed.
   - While NeurIPS does not require releasing code, the conference does require all submissions to provide some reasonable avenue for reproducibility, which may depend on the nature of the contribution. For example
     (a) If the contribution is primarily a new algorithm, the paper should make it clear how to reproduce that algorithm.
     (b) If the contribution is primarily a new model architecture, the paper should describe the architecture clearly and fully.
     (c) If the contribution is a new model (e.g., a large language model), then there should either be a way to access this model for reproducing the results or a way to reproduce the model (e.g., with an open-source dataset or instructions for how to construct the dataset).

(d) We recognize that reproducibility may be tricky in some cases, in which case authors are welcome to describe the particular way they provide for reproducibility. In the case of closed-source models, it may be that access to the model is limited in some way (e.g., to registered users), but it should be possible for other researchers to have some path to reproducing or verifying the results.

5. **Open access to data and code**

   Question: Does the paper provide open access to the data and code, with sufficient instructions to faithfully reproduce the main experimental results, as described in supplemental material?

   Answer: [Yes]

   Justification: We provide the full code, data, and necessary data preprocessing pipelines to reproduce the experiments.

   Guidelines:

   - The answer NA means that paper does not include experiments requiring code.
   - Please see the NeurIPS code and data submission guidelines (`https://nips.cc/public/guides/CodeSubmissionPolicy`) for more details.
   - While we encourage the release of code and data, we understand that this might not be possible, so "No" is an acceptable answer. Papers cannot be rejected simply for not including code, unless this is central to the contribution (e.g., for a new open-source benchmark).
   - The instructions should contain the exact command and environment needed to run to reproduce the results. See the NeurIPS code and data submission guidelines (`https://nips.cc/public/guides/CodeSubmissionPolicy`) for more details.
   - The authors should provide instructions on data access and preparation, including how to access the raw data, preprocessed data, intermediate data, and generated data, etc.
   - The authors should provide scripts to reproduce all experimental results for the new proposed method and baselines. If only a subset of experiments are reproducible, they should state which ones are omitted from the script and why.
   - At submission time, to preserve anonymity, the authors should release anonymized versions (if applicable).
   - Providing as much information as possible in supplemental material (appended to the paper) is recommended, but including URLs to data and code is permitted.

6. **Experimental Setting/Details**

   Question: Does the paper specify all the training and test details (e.g., data splits, hyperparameters, how they were chosen, type of optimizer, etc.) necessary to understand the results?

   Answer: [Yes]

   Justification: The details of the data splits for each dataset used are provided in Table 8 and overview of phylogeny is given in Table 7. We also give details of key hyperparameters and the way they were chosen in Supplementary Section E. Full code also provided for reproducibility.

   Guidelines:

   - The answer NA means that the paper does not include experiments.
   - The experimental setting should be presented in the core of the paper to a level of detail that is necessary to appreciate the results and make sense of them.
   - The full details can be provided either with the code, in appendix, or as supplemental material.

7. **Experiment Statistical Significance**

   Question: Does the paper report error bars suitably and correctly defined or other appropriate information about the statistical significance of the experiments?

   Answer: [Yes]

Justification: We have done multiple runs of our model on Bird dataset with different random weight initialization, and report the mean and standard deviation of accuracy in Supplementary Section D

Guidelines:

- The answer NA means that the paper does not include experiments.
- The authors should answer "Yes" if the results are accompanied by error bars, confidence intervals, or statistical significance tests, at least for the experiments that support the main claims of the paper.
- The factors of variability that the error bars are capturing should be clearly stated (for example, train/test split, initialization, random drawing of some parameter, or overall run with given experimental conditions).
- The method for calculating the error bars should be explained (closed form formula, call to a library function, bootstrap, etc.)
- The assumptions made should be given (e.g., Normally distributed errors).
- It should be clear whether the error bar is the standard deviation or the standard error of the mean.
- It is OK to report 1-sigma error bars, but one should state it. The authors should preferably report a 2-sigma error bar than state that they have a 96% CI, if the hypothesis of Normality of errors is not verified.
- For asymmetric distributions, the authors should be careful not to show in tables or figures symmetric error bars that would yield results that are out of range (e.g. negative error rates).
- If error bars are reported in tables or plots, The authors should explain in the text how they were calculated and reference the corresponding figures or tables in the text.

8. **Experiments Compute Resources**

   Question: For each experiment, does the paper provide sufficient information on the computer resources (type of compute workers, memory, time of execution) needed to reproduce the experiments?

   Answer: [Yes]

   Justification: Details of computer resources used are provided in Supplementary Section E

   Guidelines:

   - The answer NA means that the paper does not include experiments.
   - The paper should indicate the type of compute workers CPU or GPU, internal cluster, or cloud provider, including relevant memory and storage.
   - The paper should provide the amount of compute required for each of the individual experimental runs as well as estimate the total compute.
   - The paper should disclose whether the full research project required more compute than the experiments reported in the paper (e.g., preliminary or failed experiments that didn't make it into the paper).

9. **Code Of Ethics**

   Question: Does the research conducted in the paper conform, in every respect, with the NeurIPS Code of Ethics `https://neurips.cc/public/EthicsGuidelines`?

   Answer: [Yes]

   Justification: The work abides by NeurIPS Code of Ethics in every aspect.

   Guidelines:

   - The answer NA means that the authors have not reviewed the NeurIPS Code of Ethics.
   - If the authors answer No, they should explain the special circumstances that require a deviation from the Code of Ethics.
   - The authors should make sure to preserve anonymity (e.g., if there is a special consideration due to laws or regulations in their jurisdiction).

10. **Broader Impacts**

Question: Does the paper discuss both potential positive societal impacts and negative societal impacts of the work performed?

Answer: [NA]

Justification: There is no negative societal impact of the work performed to the best of our knowledge.

Guidelines:

- The answer NA means that there is no societal impact of the work performed.
- If the authors answer NA or No, they should explain why their work has no societal impact or why the paper does not address societal impact.
- Examples of negative societal impacts include potential malicious or unintended uses (e.g., disinformation, generating fake profiles, surveillance), fairness considerations (e.g., deployment of technologies that could make decisions that unfairly impact specific groups), privacy considerations, and security considerations.
- The conference expects that many papers will be foundational research and not tied to particular applications, let alone deployments. However, if there is a direct path to any negative applications, the authors should point it out. For example, it is legitimate to point out that an improvement in the quality of generative models could be used to generate deepfakes for disinformation. On the other hand, it is not needed to point out that a generic algorithm for optimizing neural networks could enable people to train models that generate Deepfakes faster.
- The authors should consider possible harms that could arise when the technology is being used as intended and functioning correctly, harms that could arise when the technology is being used as intended but gives incorrect results, and harms following from (intentional or unintentional) misuse of the technology.
- If there are negative societal impacts, the authors could also discuss possible mitigation strategies (e.g., gated release of models, providing defenses in addition to attacks, mechanisms for monitoring misuse, mechanisms to monitor how a system learns from feedback over time, improving the efficiency and accessibility of ML).

11. **Safeguards**

Question: Does the paper describe safeguards that have been put in place for responsible release of data or models that have a high risk for misuse (e.g., pretrained language models, image generators, or scraped datasets)?

Answer: [NA]

Justification: The work poses no risk of misuse.

Guidelines:

- The answer NA means that the paper poses no such risks.
- Released models that have a high risk for misuse or dual-use should be released with necessary safeguards to allow for controlled use of the model, for example by requiring that users adhere to usage guidelines or restrictions to access the model or implementing safety filters.
- Datasets that have been scraped from the Internet could pose safety risks. The authors should describe how they avoided releasing unsafe images.
- We recognize that providing effective safeguards is challenging, and many papers do not require this, but we encourage authors to take this into account and make a best faith effort.

12. **Licenses for existing assets**

Question: Are the creators or original owners of assets (e.g., code, data, models), used in the paper, properly credited and are the license and terms of use explicitly mentioned and properly respected?

Answer: [Yes]

Justification: All datasets used have been cited along with their source wherever necessary. We also mention the license details for each dataset used in Supplementary Section E

Guidelines:

- The answer NA means that the paper does not use existing assets.
- The authors should cite the original paper that produced the code package or dataset.
- The authors should state which version of the asset is used and, if possible, include a URL.
- The name of the license (e.g., CC-BY 4.0) should be included for each asset.
- For scraped data from a particular source (e.g., website), the copyright and terms of service of that source should be provided.
- If assets are released, the license, copyright information, and terms of use in the package should be provided. For popular datasets, `paperswithcode.com/datasets` has curated licenses for some datasets. Their licensing guide can help determine the license of a dataset.
- For existing datasets that are re-packaged, both the original license and the license of the derived asset (if it has changed) should be provided.
- If this information is not available online, the authors are encouraged to reach out to the asset's creators.

13. **New Assets**

    Question: Are new assets introduced in the paper well documented and is the documentation provided alongside the assets?

    Answer: [Yes]

    Justification: We provide the full code and the necessary documentation to reproduce the results.

    Guidelines:

    - The answer NA means that the paper does not release new assets.
    - Researchers should communicate the details of the dataset/code/model as part of their submissions via structured templates. This includes details about training, license, limitations, etc.
    - The paper should discuss whether and how consent was obtained from people whose asset is used.
    - At submission time, remember to anonymize your assets (if applicable). You can either create an anonymized URL or include an anonymized zip file.

14. **Crowdsourcing and Research with Human Subjects**

    Question: For crowdsourcing experiments and research with human subjects, does the paper include the full text of instructions given to participants and screenshots, if applicable, as well as details about compensation (if any)?

    Answer: [NA]

    Justification: No crowdsourcing or human subject involved in this research.

    Guidelines:

    - The answer NA means that the paper does not involve crowdsourcing nor research with human subjects.
    - Including this information in the supplemental material is fine, but if the main contribution of the paper involves human subjects, then as much detail as possible should be included in the main paper.
    - According to the NeurIPS Code of Ethics, workers involved in data collection, curation, or other labor should be paid at least the minimum wage in the country of the data collector.

15. **Institutional Review Board (IRB) Approvals or Equivalent for Research with Human Subjects**

    Question: Does the paper describe potential risks incurred by study participants, whether such risks were disclosed to the subjects, and whether Institutional Review Board (IRB) approvals (or an equivalent approval/review based on the requirements of your country or institution) were obtained?

    Answer: [NA]

Justification: No crowdsourcing or human subject involved in this research.

Guidelines:

- The answer NA means that the paper does not involve crowdsourcing nor research with human subjects.
- Depending on the country in which research is conducted, IRB approval (or equivalent) may be required for any human subjects research. If you obtained IRB approval, you should clearly state this in the paper.
- We recognize that the procedures for this may vary significantly between institutions and locations, and we expect authors to adhere to the NeurIPS Code of Ethics and the guidelines for their institution.
- For initial submissions, do not include any information that would break anonymity (if applicable), such as the institution conducting the review.

A Ablation of Over-specificity Loss Trade-off Hyperparameter

We have provided an ablation for the over-specificity loss trade-off hyperparameter (λ_{ovsp}) in Table 4. We can observe that increasing the weight of over-specificity loss reduces the model's classification performance, as the model struggles to find any commonality especially at internal nodes where the number of leaf descendant species are large in number and quite diverse. It is natural that species that are diverse and distantly related may share fewer characteristics with each other, in comparison to a set of species that diverged more recently from a common ancestor [14, 15]. Therefore, forcing the model to learn common traits with a strong $\mathcal{L}_{ovsp}$ constraint can cause the model to perform bad in terms of accuracy.

Table 4: Ablation of over-specificity loss trade-off hyperparameter (λ_{ovsp}). Done on Bird dataset.

λ_{ovsp}	Part purity	Part purity with mask applied	% masked	% Accuracy
w/o $\mathcal{L}_{ovsp}$	0.68 ± 0.22	0.75 ± 0.17	21.42%	58.32
0.05	$\mathbf{0.72 \pm 0.19}$	$\mathbf{0.77 \pm 0.16}$	16.53%	70.01
0.1	0.71 ± 0.18	0.74 ± 0.16	11.31%	**70.97**
0.5	0.71 ± 0.19	0.72 ± 0.18	4.2%	68.23
1.0	0.70 ± 0.19	0.70 ± 0.2	2.13%	62.68
2.0	0.69 ± 0.19	0.69 ± 0.19	0.55%	53.16

B Ablation of Number of Prototypes

In Table 5 we vary the number of prototypes per child β for a node to see the impact on model's performance. We note that while the accuracy increases marginally with increasing the number of prototypes per child (β) from 10 to 15, it also considerably increases the overall number of prototypes initialized. Therefore we continue to work with $\beta = 10$ for all of our experiments.

Table 5: Ablation of number of prototypes per child for a node (β). Done on Bird dataset.

Number of Prototypes (β)	% Accuracy
10	70.01
15	**70.92**
20	67.93

C Ablation of Individual Losses

In Table 6, we perform an ablation of the various loss terms used in our methodology. As it can be observed, removal of $\mathcal{L}_{ovsp}$ and $\mathcal{L}_{disc}$ degrades performance in terms of both semantic consistency (part purity) and accuracy. On the other hand, removal of self supervised contrastive loss $\mathcal{L}_{SS}$ improves accuracy but at the cost of drastically decreasing the semantic consistency.

Table 6: Ablation of individual losses. Done on Bird dataset.

Model	Part purity	Part purity with mask applied	% masked	% Accuracy
HComP-Net	0.72 ± 0.19	0.77 ± 0.16	16.53%	70.01
HComP-Net w/o $\mathcal{L}_{ovsp}$	0.68 ± 0.22	0.75 ± 0.17	21.42%	58.32
HComP-Net w/o $\mathcal{L}_{disc}$	0.69 ± 0.19	0.72 ± 0.17	10.95%	65.99
HComP-Net w/o $\mathcal{L}_{SS}$	0.53 ± 0.18	0.57 ± 0.15	8.36%	81.62

D Consistency of Classification Performance Over Multiple Runs

We trained the model using five distinct random weight initializations. The results showed that the model's fine-grained accuracy averaged 70.63% with a standard deviation of 0.18%.

E Implementation Details

We have included all the source code and dataset along with the comprehensive instructions to reproduce the results, in the supplementary material (.zip file).

Model hyper-parameters: We build HComP-Net on top of a ConvNeXt-tiny architecture as the backbone feature extractor. We have modified the stride of the max pooling layers of later stages of the backbone from 2 to 1 similar to PIP-Net such that the backbone produces feature maps of increased height and width, in order to get more fine-grained prototype score maps. We implement and experiment our method on ConvNeXt-tiny backbones with 26×26 feature maps. The length of prototype vectors C is 768. The weights ϕ at every node n of HComP-Net are constrained to be non-negative by the use of ReLU activation function [56]. Further, the prototype activation nodes are connected with non-negative weights only to their respective child classes in W while their weights to other classes are made zero and non-trainable.

Training details: All models were trained with images resized and appropriately padded to 224×224 pixel resolution and augmented using TrivialAugment [57] for contrastive learning. The prototypes are pretrained with self-supervised learning similar to PIP-Net for 10 epochs, following which the model is trained with the entire set of loss functions for 60 epochs. We use a batch size of 256 for Bird dataset and 64 for Butterfly and Fish dataset. The masking module is trained in parallel and its training is continued for 15 additional epochs after the training of rest of the model is completed. The trade-off hyper-parameters for the loss functions are set to be $\lambda_{CE} = 2; \lambda_A = 5; \lambda_T = 2; \lambda_{ovsp} = 0.05; \lambda_{disc} = 0.1; \lambda_{orth} = 0.1; \lambda_{mask} = 2.0; \lambda_{L1} = 0.5$. λ_{CE}, λ_T and λ_A were borrowed from PIP-Net [18]. Ablations to arrive at suitable λ_{ovsp} is provided in Table 4. λ_{disc} and λ_{orth} were chosen empirically and found to work well on all three datasets. Experiment on unseen species was done by leaving out certain classes from the datasets, so that they are not considered during training.

Dataset and Phylogeny Details: Dataset statistics and phylogeny statistics are provided in Table 8 and Table 7 respectively. Bird dataset is created by choosing 190 species from CUB-200-2011 [2] [8] dataset, which were part of the phylogeny. Background from all images were filtered using the associated segmentation metadata [58]. For Butterfly dataset we considered each subspecies as an individual class and considered only the subspecies of genus Heliconius from the Heliconius Collection (Cambridge Butterfly)[3] [16]. There is substantial variation among subspecies of Heliconius species. Furthermore, we balanced the dataset by filtering out the subspecies which did not have 20 or more images. We also sampled a subset of 100 images from each subspecies that had more than 100 images. For Fish [4] dataset, we followed the exact same preprocessing steps as outlined in PhyloNN [9].

Compute Resources: The models for Bird dataset were trained on two NVIDIA A100 GPUs with 80GB of RAM each. Butterfly and Fish models were trained on single A100 GPU. As a rough estimate the execution time for training model on Bird dataset is around 2.5 hours. For Butterfly and Fish datasets, the training completes under 1 hour. We used a single A100 GPU during inference stage for all other analysis.

Table 7: High level statistics of the phylogenies used for different datasets.

Phylogeny	# Internal nodes	Max-depth	Min-depth
Bird	184	25	3
Butterfly	13	5	2
Fish	20	11	2

[2] License: CC BY

[3] Note that this dataset is a compilation of images from 25 Zenodo records by the Butterfly Genetics Group at Cambridge University, licensed under Creative Commons Attribution 4.0 International ([27, 28, 29, 30, 31, 32, 33, 34, 35, 36, 37, 38, 39, 40, 41, 42, 43, 44, 45, 46, 47, 48, 49, 50, 51]).

[4] License: CC BY-NC

Table 8: Dataset statistics (# train and validation images).

Dataset	# Classes	Train set	Validation set
Bird	190	5695	5512
Butterfly	30	1418	358
Fish	38	4140	1294

Table 9: Part purity with post-hoc thresholding approach. Done on **Bird** dataset.

Threshold	Part purity with mask applied	% masked
0.2	0.74 ± 0.28	12.28%
0.3	0.75 ± 0.27	13.47%
0.4	0.76 ± 0.26	14.97%
0.5	0.77 ± 0.15	16.66%
0.6	0.77 ± 0.26	17.43%

F Post-hoc Thresholding to Identify Over-specific Prototypes

An alternative approach to learning masking module is to calculate the over-specificity score for each prototype on the test set after training the model. We calculate the over-specificity scores for the prototypes of a trained model as follows,

$$\mathcal{O}_i = -\prod_{d=1}^{D_i} \frac{1}{\text{top}_k} \sum_{i=1}^{\text{top}_k} (\mathbf{g_i}) \tag{9}$$

For a given prototype, we choose the top_k images with the highest prototype scores from each leaf descendant. After taking mean of the top_k prototype score, we multiply the values from each descendant to arrive at the over-specificity score for the particular prototype. Subsequently we choose a threshold to determine which prototypes are over-specific. We provide the results of post-hoc thresholding approach that can also be used to identify overspecific prototypes in Table 9. While we can note that this approach can also be effective, validating the threshold particularly in scenarious where there is no part annotations available (such as part location annotation of CUB-200-2011) can be an ardous task. In such cases directly identifying over-specific prototypes as part of the training through masking module can be the more feasible option.

G Additional Visualizations of the Hierarchical Prototypes Discovered by HComP-Net

We provide more visualizations of the hierarchical prototypes discovered by HComP-Net for Butterfly (Figures 7 and 8) and Fish (Figure 9) datasets in this section. For ease of visualization, in each figure we visualize the prototypes learned over a small sub-tree from the phylogeny. The prototypes at the lowest level capture traits that are species-specific whereas the prototypes at internal nodes capture the commonality between its descendant species. For Fish dataset, we have provided textual descriptions purely based on human interpretation for the traits that are captured by prototypes at different levels. For Butterfly dataset, since the prototypes are capturing different wing patterns, assigning textual description for them is not straightforward. Therefore, we refrain from providing any text description for the highlighted regions of the learned prototypes and leave it to the reader's interpretation.

H Additional Top-K Visualizations of HComP-Net Prototypes

We provide additional top-K visualizations of the prototypes from Butterfly (Figures 10 to 13) and Fish (Figures 14 to 16) datasets, where every row corresponds to a descendant species and the columns corresponds to the top-K images from the species with the largest prototype activation scores. A requirement of a semantically meaningful prototype is that it should consistently highlight the same part of the organisms in various images, provided that the part is visible. We can see in the

figures that the prototypes learned by HComP-Net consistently highlight the same part across all top-K images of a species, and across all descendant species. We additionally show that HComP-Net can find common traits at internal nodes with varying number of descendant species, including 4 species (Figure 10), 5 species (Figures 11 and 12), and 10 species (Figure 13) of butterflies, and 5 species (Figure 14), 8 species (Figure 15) and 18 species (Figure 16) for fish. We also provide several top-k visualizations of prototypes learned for bird species in Figures 17 to 25. This shows the ability of HComP-Net to discover common prototypes at internal nodes of the phylogenetic tree that consistently highlight the same regions in the descendant species images even when the number of descendants is large.

I Limitations of Our Work

A fundamental challenge of every prototype-based interpretability method (including ours) is the difficulty in associating a semantic interpretation to the underlying visual concept of a prototype. While some prototypes can be interpreted easily based on visual inspection of prototype activation maps, other prototypes are harder to interpret and require additional domain expertise of biologists. Also, while we have considered large phylogenies as that of the 190 species from CUB dataset, it may still not be representative of all bird species. This limited scope may cause our method to identify apparent homologous evolutionary traits that could differ with the inclusion of more species into the phylogeny. Therefore, our method can be seen as a system that generates potential hypotheses about evolutionary traits discovered in the form of hierarchical prototypes.

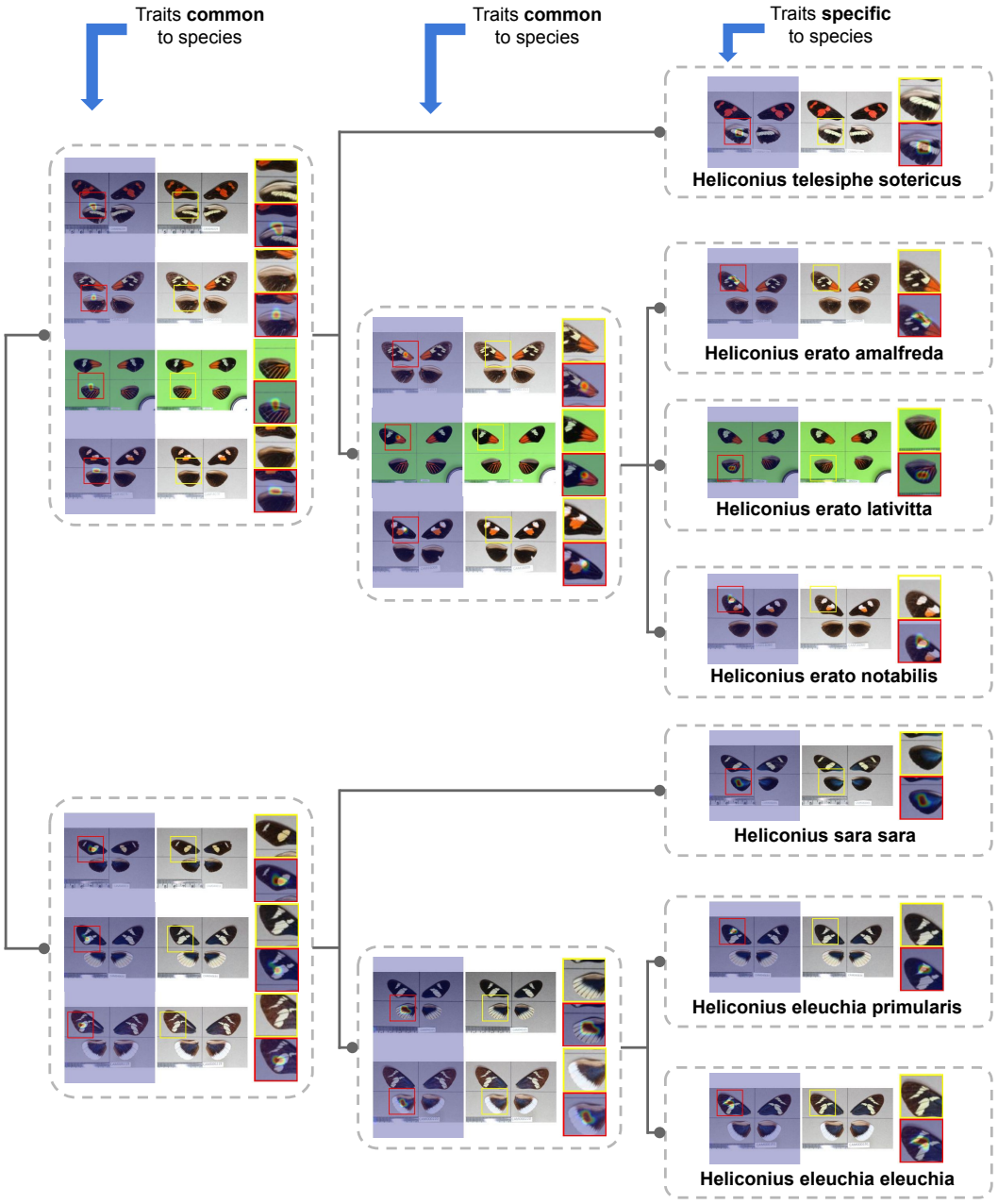

Figure 7: Visualizing the hierarchy of prototypes discovered by HComP-Net over three levels in the phylogeny of seven species from **Butterfly** dataset. For each prototype we visualize one image from each of its leaf descendant. Therefore, for prototypes at species level (rightmost column) we show only one image whereas for prototypes at internal nodes we show multiple images (equal to the number of leaf descendants). For each image, we show the zoomed in view of the original image as well as the heatmap overlayed image in the region of the learned prototype. The prototypes appear to be capturing different wing patterns of the butterflies.

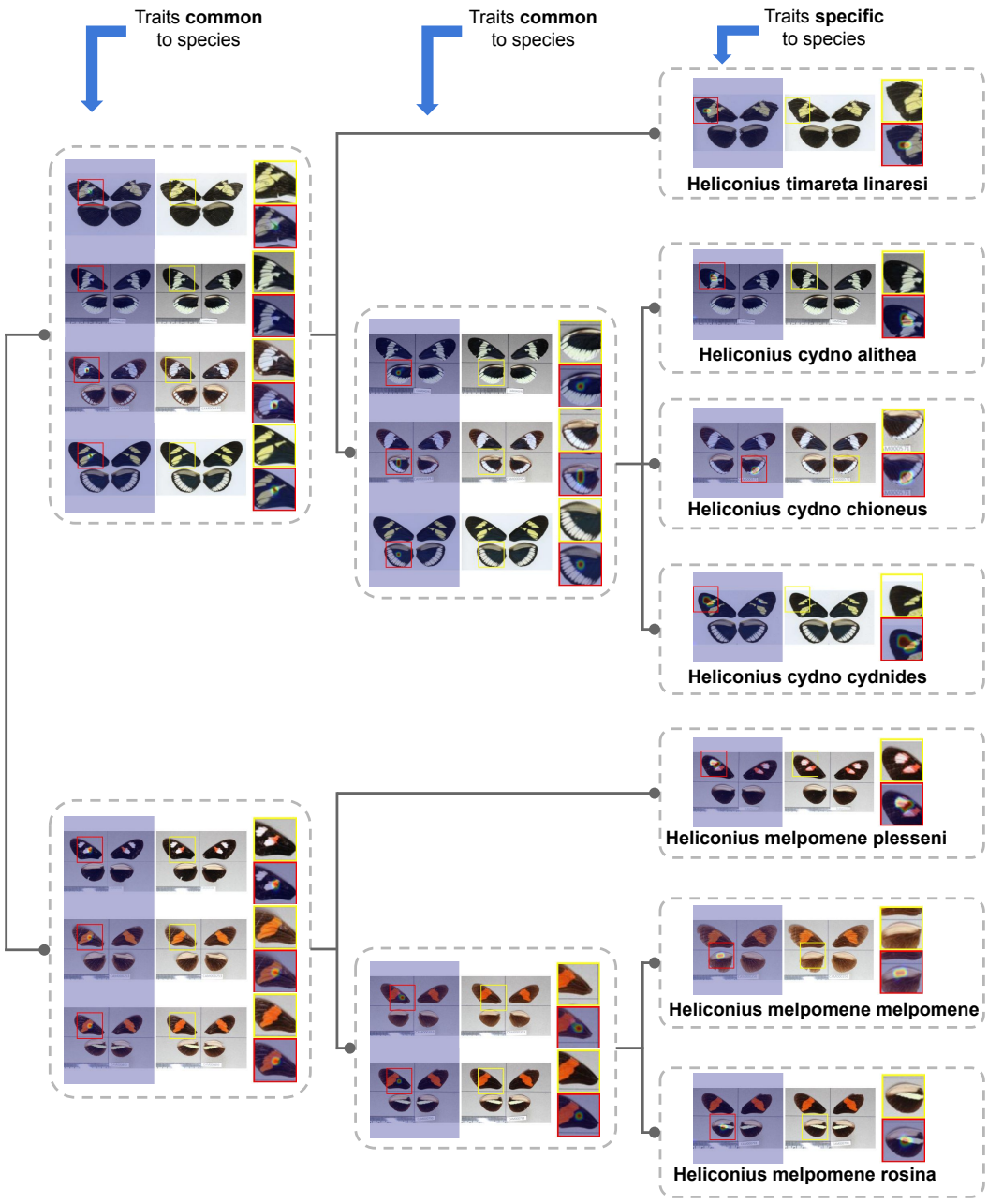

Figure 8: Visualizing the hierarchy of prototypes discovered by HComP-Net over three levels in the phylogeny of seven species from **Butterfly** dataset.

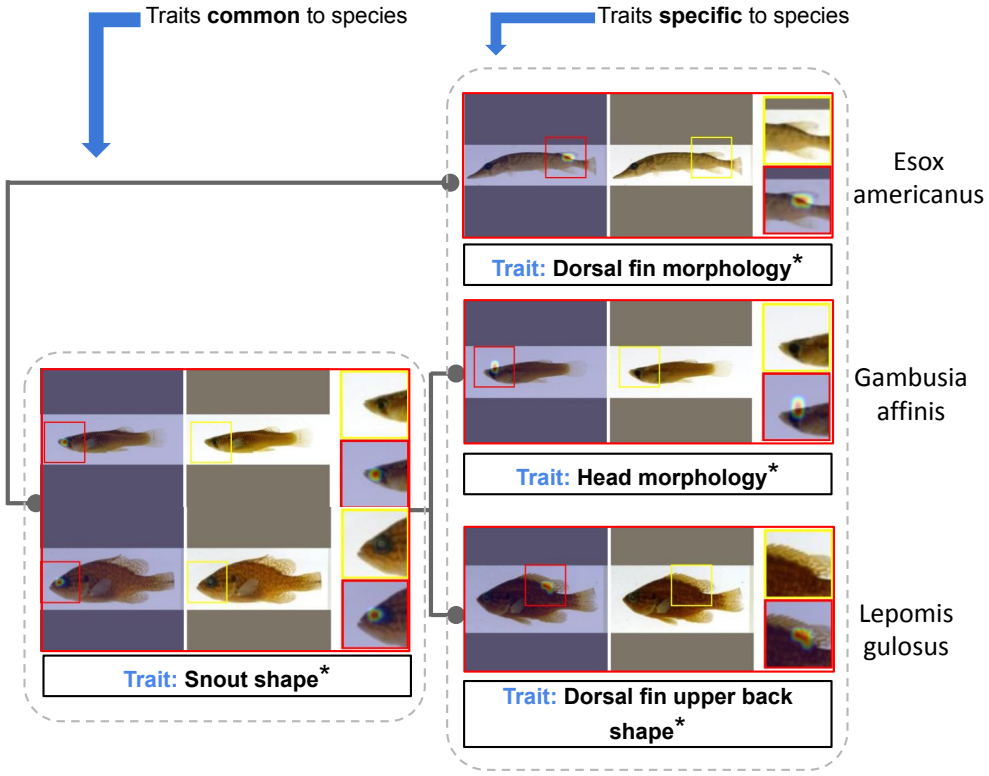

Figure 9: Visualizing the hierarchy of prototypes discovered by HComP-Net for a sub-trees with three species from **Fish** dataset. *Note that the textual descriptions of the hypothesized traits shown for every prototype are based on human interpretation.

Figure 10: Top-K visualization of a prototype finding commonality between four species of butterfly sharing a common ancestor. Each row represents the top 3 images from the respective species. For each image we show the zoomed in view of the original image as well as the heatmap overlayed image.

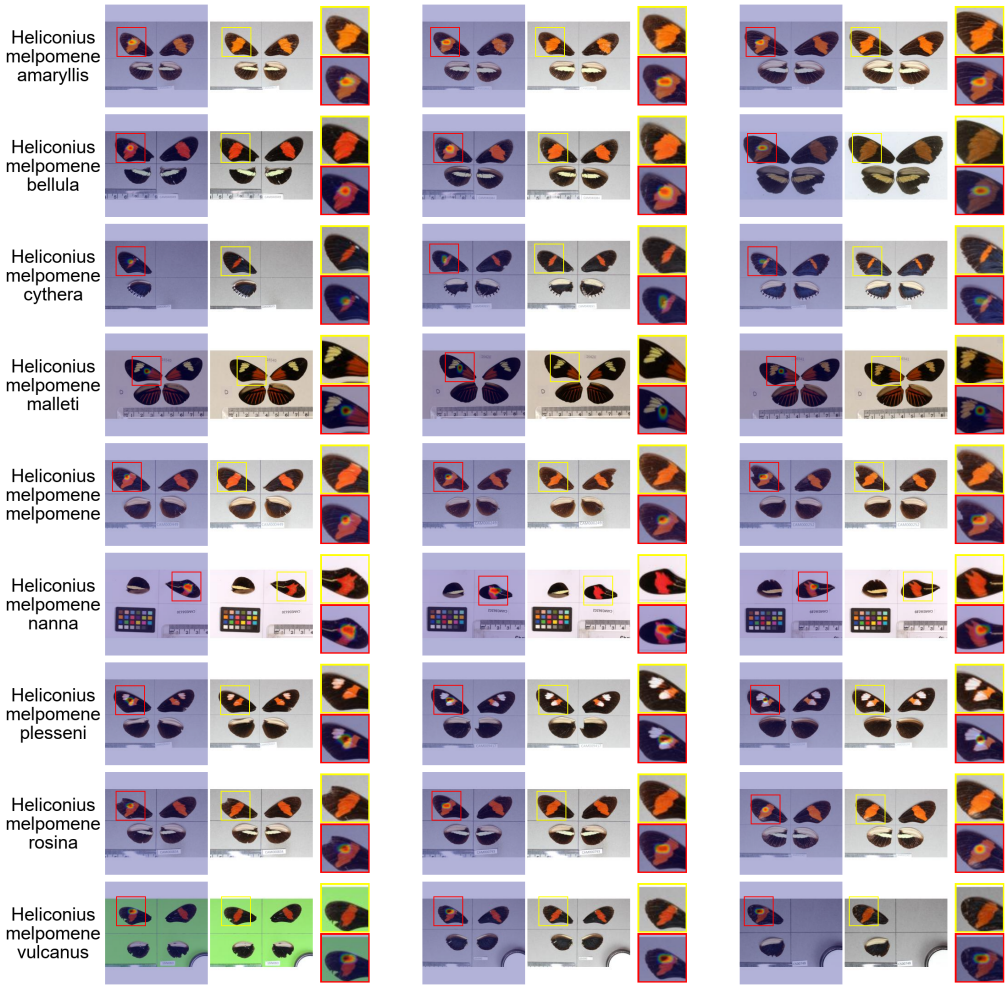

Figure 11: Top-K visualization of a prototype finding commonality between nine species of butterfly sharing a common ancestor. Each row represents the top 3 images from the respective species. For each image we show the zoomed in view of the original image as well as the heatmap overlayed image.

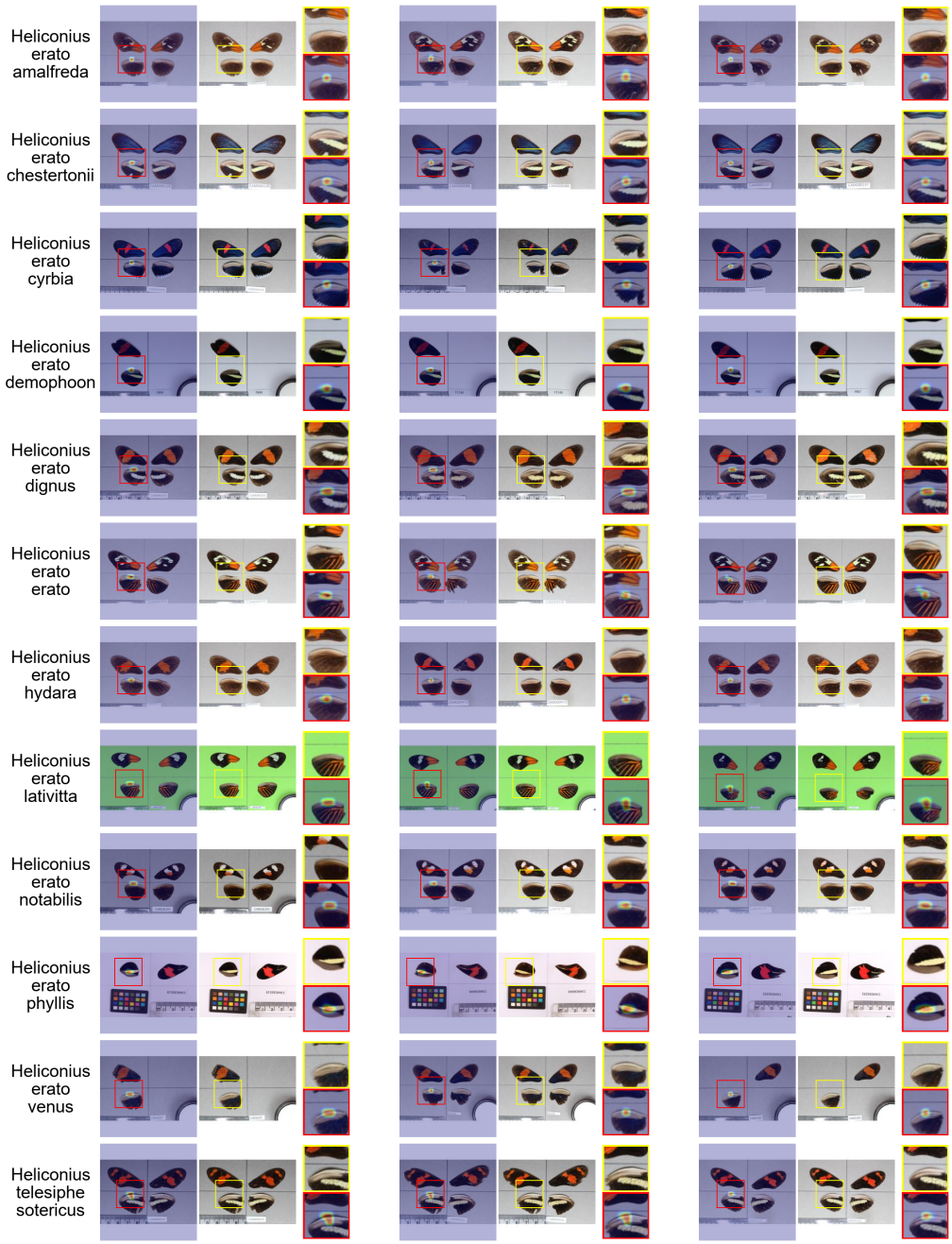

Figure 12: Top-K visualization of a prototype finding commonality between twelve species of butterfly sharing a common ancestor. Each row represents the top 3 images from the respective species. For each image we show the zoomed in view of the original image as well as the heatmap overlayed image.

Figure 13: Top-K visualization of a prototype finding commonality between four species of butterfly sharing a common ancestor. Each row represents the top 3 images from the respective species. For each image we show the zoomed in view of the original image as well as the heatmap overlayed image.

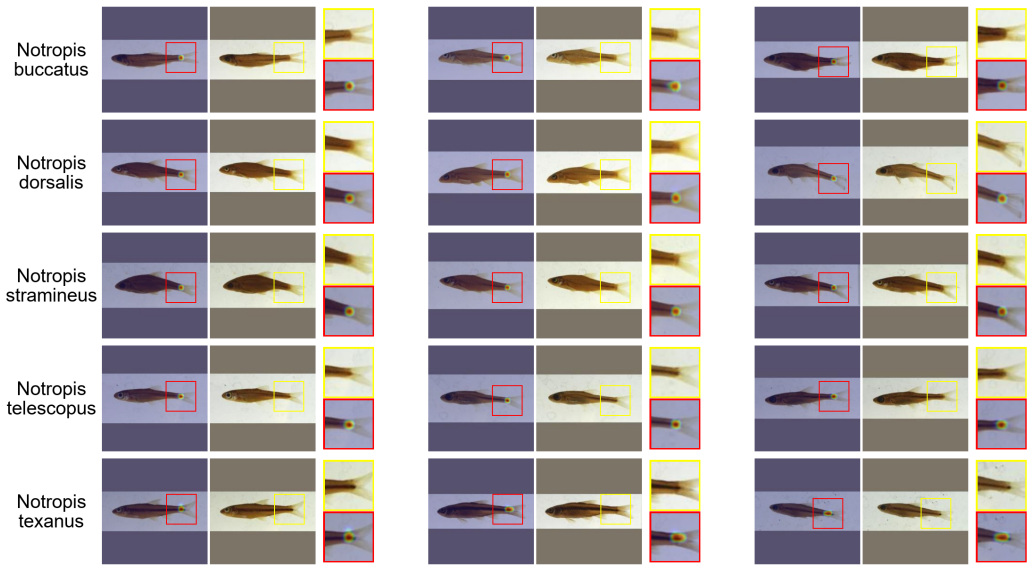

Figure 14: Top-K visualization of a prototype finding commonality between five species of fish sharing a common ancestor. Each row represents the top 3 images from the respective species. For each image we show the zoomed in view of the original image as well as the heatmap overlayed image.

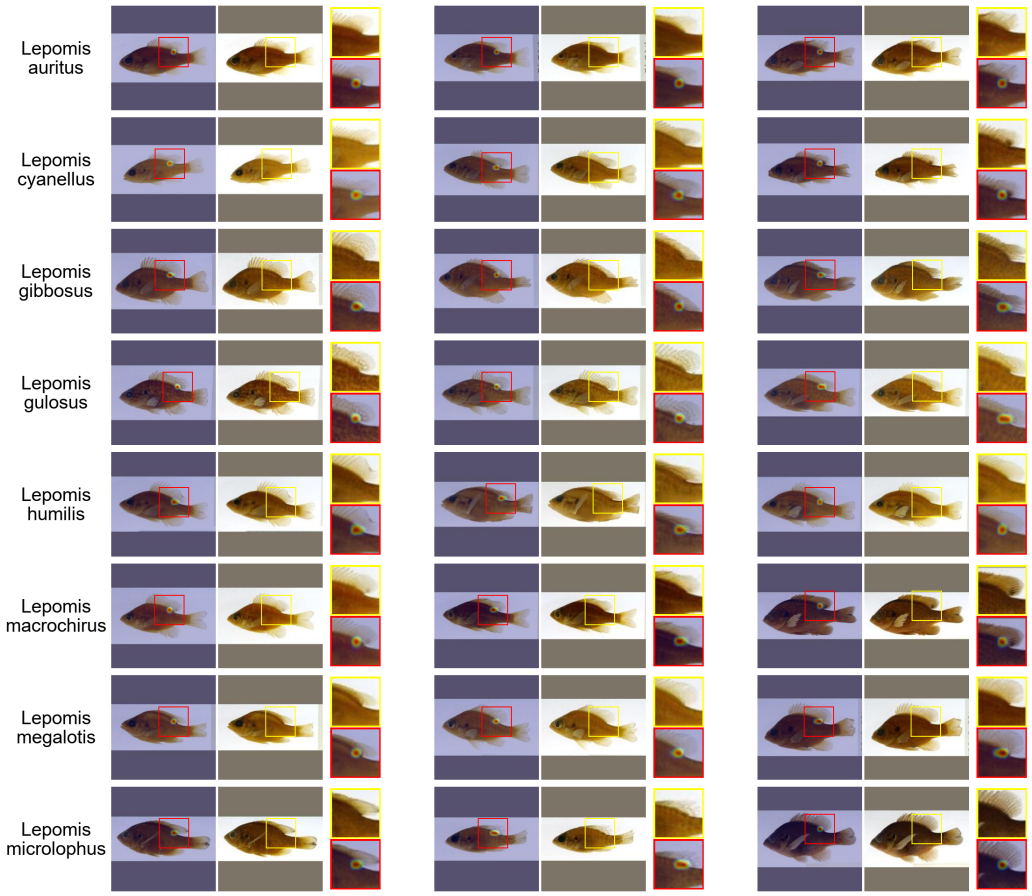

Figure 15: Top-K visualization of a prototype finding commonality between eight species of fish sharing a common ancestor. Each row represents the top 3 images from the respective species. For each image we show the zoomed in view of the original image as well as the heatmap overlayed image.

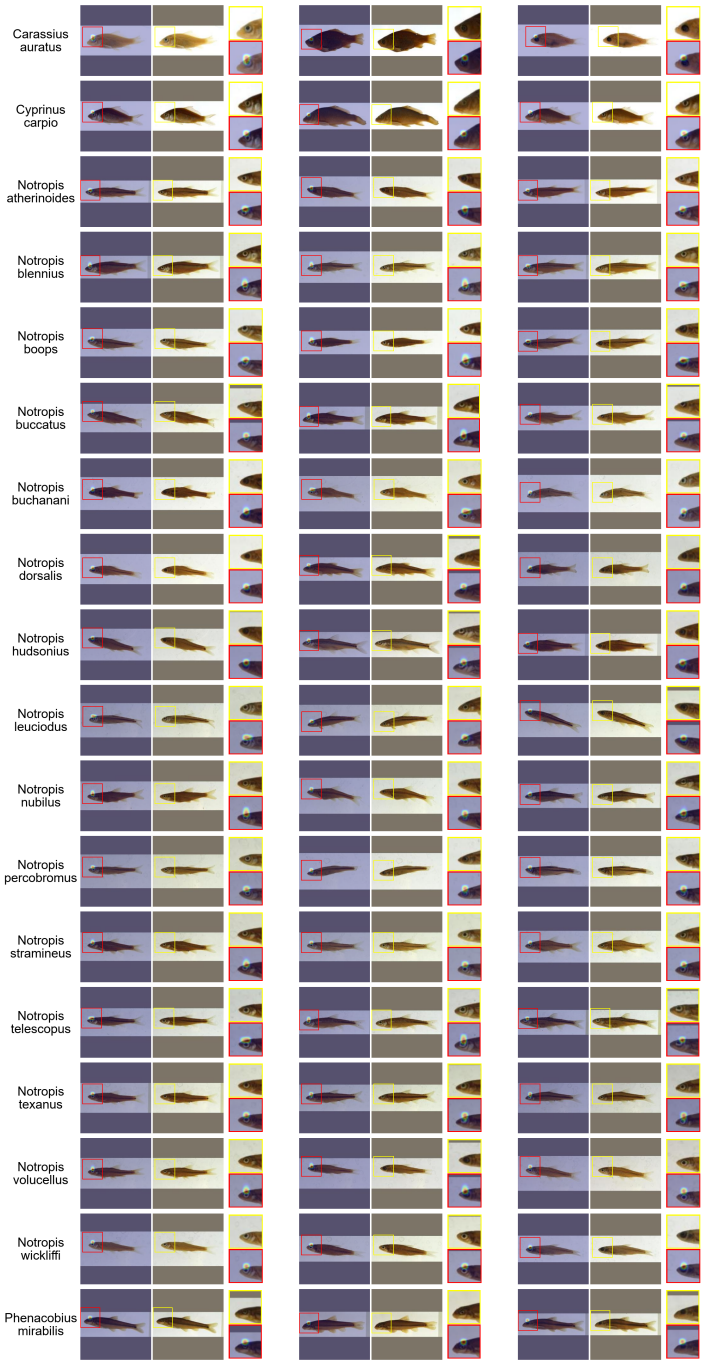

Figure 16: Top-K visualization of a prototype finding commonality between eighteen species of fish sharing a common ancestor. Each row represents the top 3 images from the respective species. For each image we show the zoomed in view of the original image as well as the heatmap overlayed image.

Figure 17: Top-K visualization of a prototype finding commonality between seven species of birds sharing a common ancestor. Each row represents the top 3 images from the respective species. For each image we show the zoomed in view of the original image as well as the heatmap overlayed image.

Figure 18: Top-K visualization of a prototype finding commonality between eight species of birds sharing a common ancestor. Each row represents the top 3 images from the respective species. For each image we show the zoomed in view of the original image as well as the heatmap overlayed image.

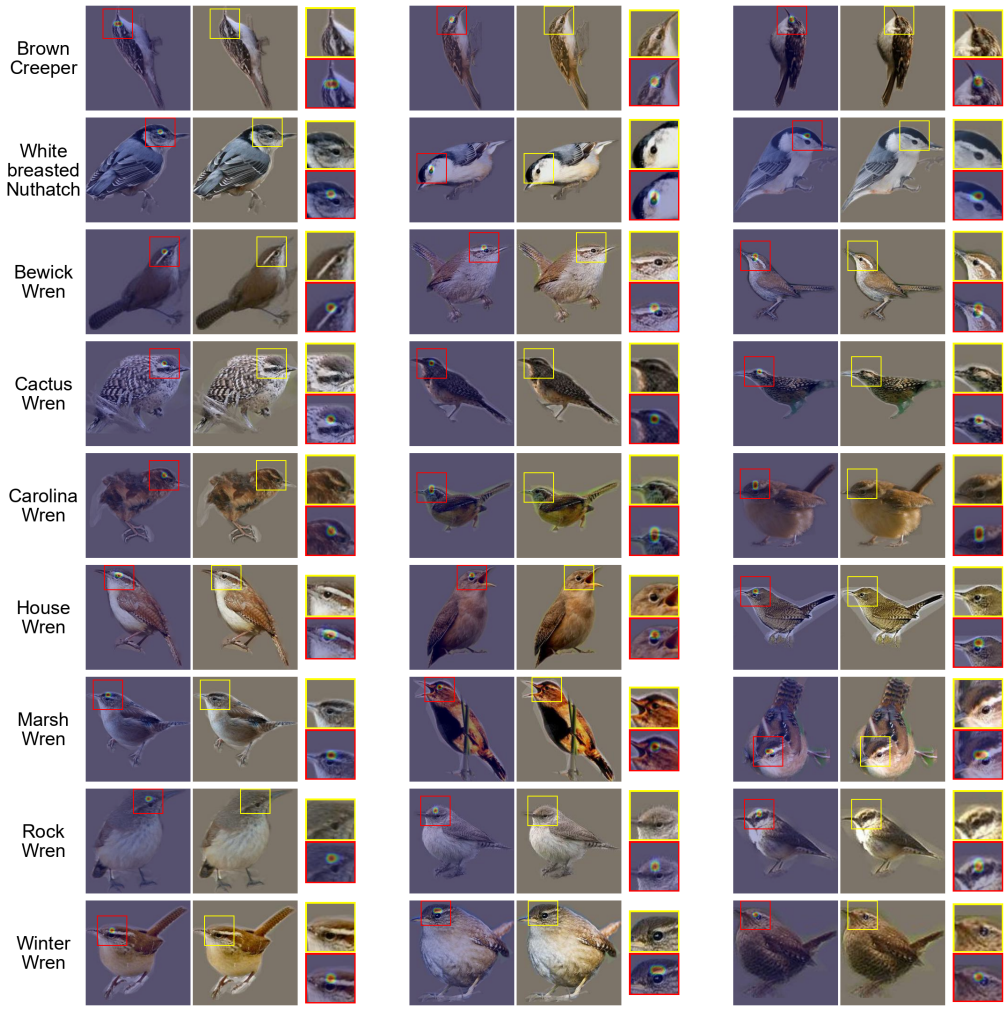

Figure 19: Top-K visualization of a prototype finding commonality between nine species of birds sharing a common ancestor. Each row represents the top 3 images from the respective species. For each image we show the zoomed in view of the original image as well as the heatmap overlayed image.

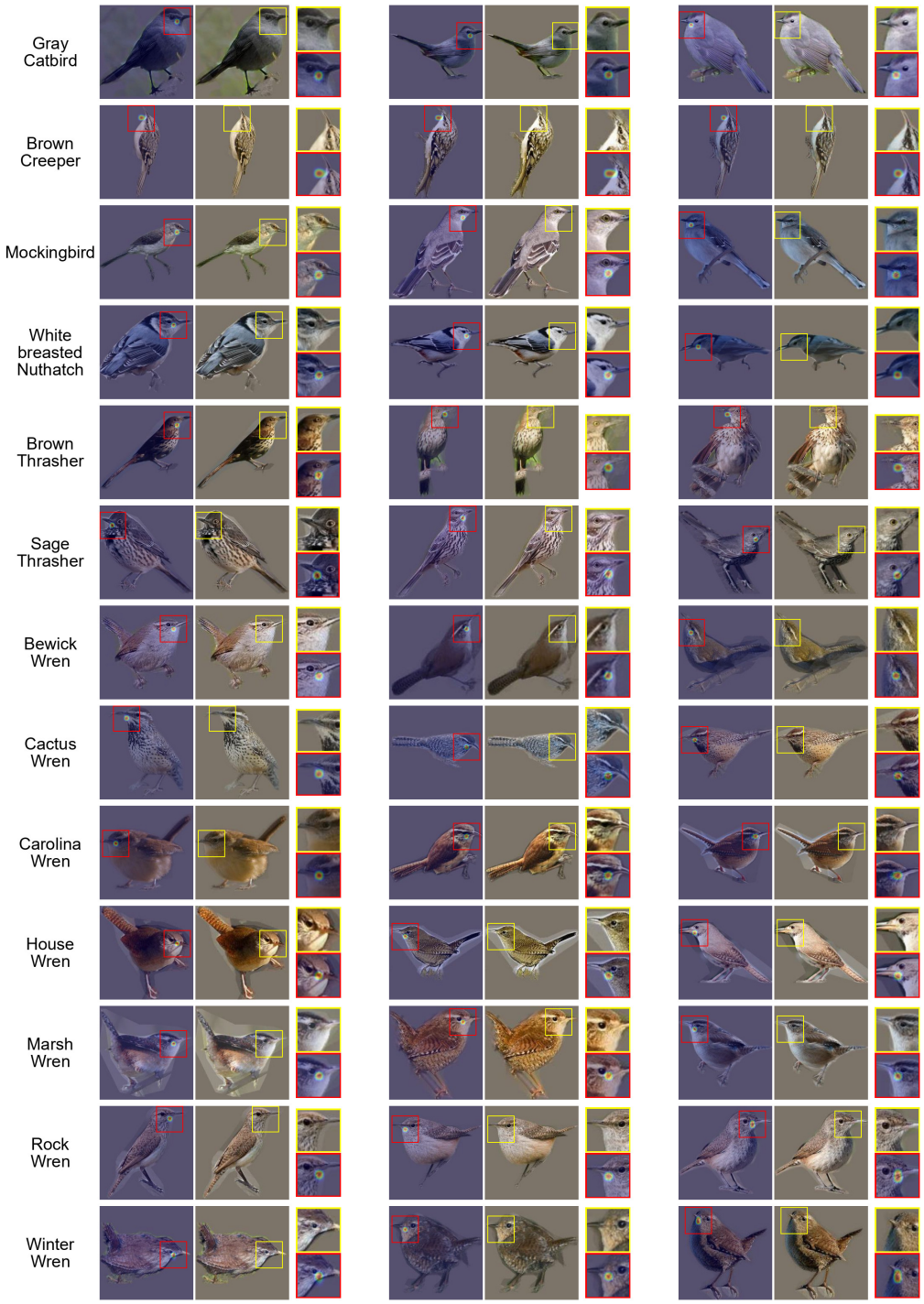

Figure 20: Top-K visualization of a prototype finding commonality between thirteen species of birds sharing a common ancestor. Each row represents the top 3 images from the respective species. For each image we show the zoomed in view of the original image as well as the heatmap overlayed image.

Figure 21: Top-K visualization of a prototype finding commonality between five species of birds sharing a common ancestor. Each row represents the top 3 images from the respective species. For each image we show the zoomed in view of the original image as well as the heatmap overlayed image.

Figure 22: Top-K visualization of a prototype finding commonality between five species of birds sharing a common ancestor. Each row represents the top 3 images from the respective species. For each image we show the zoomed in view of the original image as well as the heatmap overlayed image.

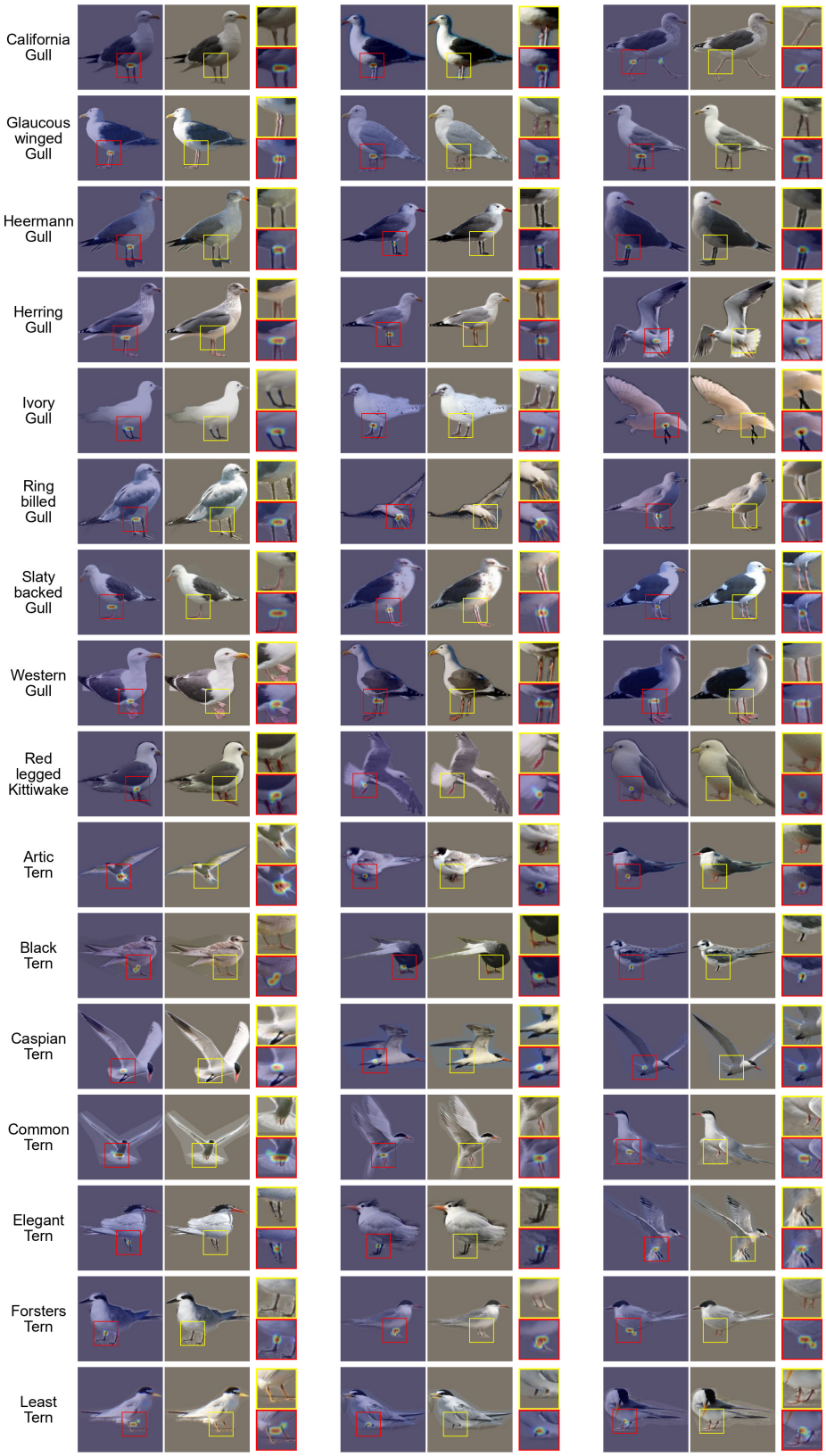

Figure 23: Top-K visualization of a prototype finding commonality between sixteen species of birds sharing a common ancestor. Each row represents the top 3 images from the respective species. For each image we show the zoomed in view of the original image as well as the heatmap overlayed image.

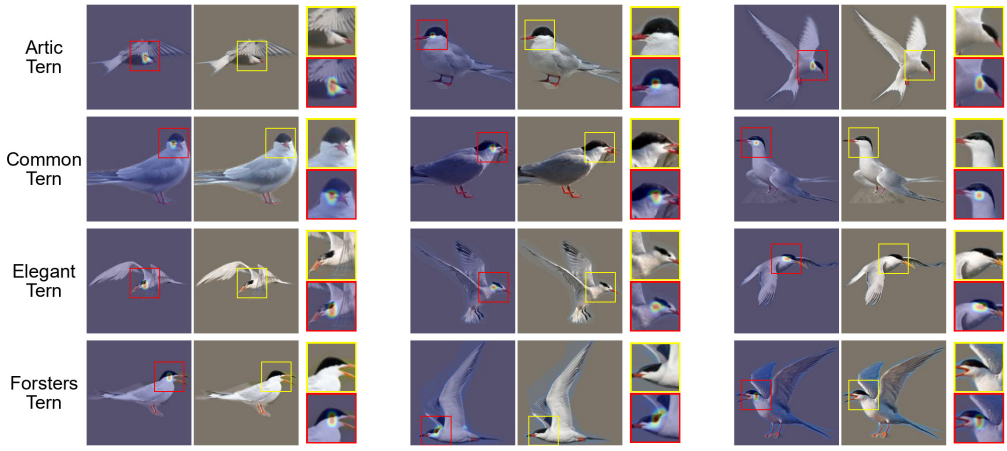

Figure 24: Top-K visualization of a prototype finding commonality between four species of birds sharing a common ancestor. Each row represents the top 3 images from the respective species. For each image we show the zoomed in view of the original image as well as the heatmap overlayed image.

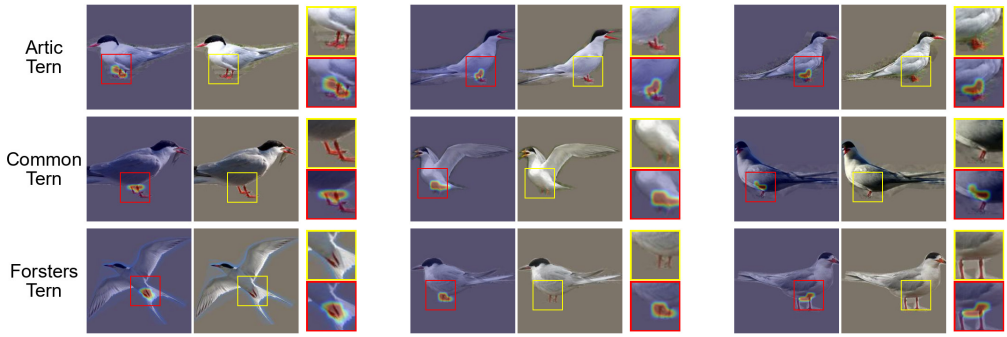

Figure 25: Top-K visualization of a prototype finding commonality between three species of birds sharing a common ancestor. Each row represents the top 3 images from the respective species. For each image we show the zoomed in view of the original image as well as the heatmap overlayed image.